VOLUME 23, 1961/62, No. 11 pp. 325-364 Published 12th September 1962

Philips Technical Review

DEALING WITH TECHNICAL PROBLEMS
RELATING TO THE PRODUCTS, PROCESSES AND INVESTIGATIONS OF
THE PHILIPS INDUSTRIES

THE NEUTRON TUBE, A SIMPLE AND COMPACT NEUTRON SOURCE

by O. REIFENSCHWEILER *) and K. NIENHUIS **).

621.387:539.125.5

In recent years the rapid expansion of nuclear physics and its practical applications, and the central rôle of the neutron in that branch of physics, have occasioned a wide demand for neutron sources. A great variety of neutron sources and generators exists, but no simple, compact, transportable type generating fast, monochromatic neutrons has been available until now. The present article deals with a sealed neutron tube that fills this gap. In some details of design and operation it resembles an X-ray tube, and it is capable of providing a continuous output of at least 10^8 neutrons per second. It is interesting to note that F. M. Penning, whose name is familiar in connection with the vacuum gauge he invented, built an experimental neutron tube as long ago as 1937, but did not follow up this line of development.

The rapid expansion of nuclear physics is due in great measure to the research into the properties of the neutron and into its interaction with matter that has been conducted all over the world, with more and more elaborate equipment, ever since this elementary particle was first discovered in 1932. So important are the applications of nuclear physics developed in recent decades that a new discipline, nuclear engineering, has come upon the scene; here too, the neutron may be said to take a central position. In a nuclear reactor the neutron is the agent that causes fission and transmits the fission reaction from one nucleus to another and, in virtue of this chain of reactions, liberates energy. Neutrons can be used to produce many of the radioactive isotopes needed as tracer elements in the study of industrial, chemical or biological processes. Crystal structures and the properties of materials can be investigated by means of neutrons, and there are many further uses for these particles.

Inquiry into the properties of neutrons, and experimental work with the aid of neutrons, are therefore important aspects nowadays of research in many fields; this kind of work invariably calls for neutron sources. The present article describes the general make-up and functioning of a sealed-off neutron source which in construction and operation resembles an X-ray tube. The development of the neutron tube in the Philips Research Laboratories ¹) can be regarded as a resumption of the work of F. M. Penning ²) in 1937; in the last few years the development has reached the stage at which, in co-operation with the Electron Tubes Division, it was ripe for quantity production. Its potential applications are reviewed at the end of the article.

Nuclear reactions yielding neutrons; neutron sources

Since, in general, neutrons exist only as component parts of atomic nuclei they can only be freed by way of nuclear reactions. Essentially, then, neutron sources are devices for staging suitable nuclear reactions. A beam of fast, lightweight nuclei (protons, deuterons or α particles) can be used for this purpose. Nuclei must be brought into close proximity if they are to react. This means overcoming the repulsion between the nuclei due to their electrical charges

---

*) Philips Research Laboratories, Eindhoven.
**) Electron Tubes Division, Philips, Eindhoven.

¹) An earlier stage of this work was reported on at the Deutsche Physikertagung 1957, held in Heidelberg. See O. Reifenschweiler and A. C. van Dorsten, Eine abgeschmolzene. Neutronenröhre, Phys. Verh. (Mosbach) **8**, 163, 1957. For *in extenso* treatment of all the problems and their solution, see O. Reifenschweiler, Philips Res. Repts **16**, 401-418, 1961 (No. 5). See also Nucleonics **18**, No. 12, 69-71, 1960.

²) F. M. Penning and J. H. A. Moubis, Eine Neutronenröhre ohne Pumpvorrichtung, Physica **4**, 1190-1199, 1937.

(Coulomb field); their velocity relative to each other must therefore be high. The relative velocity and hence the kinetic energy the particles must have are dependent on the reaction it is desired to bring about.

Three of the many types of neutron-yielding nuclear reactions may be cited here. Firstly, beryllium enters with an α particle into the reaction $^9\text{Be}(\alpha,\text{n})^{12}\text{C}$ or, in the more detailed notation:

$$^9_4\text{Be} + ^4_2\text{He} \rightarrow ^{12}_6\text{C} + ^1_0\text{n} + 5.65\ \text{MeV}\,. \quad . \quad (1)$$

Secondly, deuterium reacts with deuterium; known as the D-D reaction, this is written $\text{D(d,n)}^3\text{He}$, or, in the extended notation,

$$^2_1\text{H} + ^2_1\text{H} \rightarrow ^3_2\text{He} + ^1_0\text{n} + 3.26\ \text{MeV}\,. \quad . \quad (2)$$

Thirdly, the so-called D-T reaction, between deuterium and tritium, is written $\text{T(d,n)}^4\text{He}$ or

$$^3_1\text{H} + ^2_1\text{H} \rightarrow ^4_2\text{He} + ^1_0\text{n} + 17.6\ \text{MeV}\,. \quad . \quad (3)$$

In order to bring about any of these reactions it is necessary to give one of the partners a high kinetic energy and cause it to collide with the other partner. The energy of the incident particle plus the energy liberated by the reaction, as specified in the above equations, is shared between the two products of the reaction in accordance with the principles of conservation of energy and momentum. The neutron acquires most energy when it is emitted in the forward direction; when emitted in any other direction it acquires a smaller amount dependent on the angle it makes with the direction of motion of the incident particle, and on the initial energy of this particle. It is possible by collimation to obtain a beam of monoenergetic neutrons.

Reaction (1) above can easily be induced: all that is necessary is to bring a radioactive substance emitting alpha particles, radium or polonium for example, into proximity with beryllium. It was in this way that the neutron was discovered in the first place. Accordingly, the simplest neutron sources, which are also the oldest, consist of a mixture of powdered beryllium and (say) radium enclosed in a capsule. Various other combinations of α-emitters and neutron-yielding elements are in use.

Neutron sources embodying radioactive substances are simple in design and small in size, the rate at which they emit neutrons is virtually constant, and they are usually long-lived; nevertheless they have certain drawbacks as compared with other kinds of source. For one thing the neutrons supplied have a complex energy spectrum, and this is often undesirable in experimental work. Some types of radioactive neutron source are associated with a strong background of γ-radiation; a Ra-Be source, for example, emits about 10^4 γ-quanta per neutron. The neutron flux cannot be varied and it is therefore impossible to pulse the neutrons, though in many experiments a pulsed neutron supply is desirable. The source cannot be switched off, and consequently careful shielding is necessary even when it is not in use. The financial outlay climbs so steeply with the power of the source that for fluxes exceeding 10^7 neutrons/sec, other types of source are preferable.

There is no natural particulate radiation suitable for inducing reactions (2) and (3) or other nuclear reactions falling into the same category; the particles constituting one of the two partners in the reaction must therefore be artificially accelerated up to a high velocity. It is on this principle that the tube described here is based. Since 1932, the year in which Cockcroft and Walton did their pioneering experiments with artificially accelerated particles, the technique of using such beams to induce nuclear reactions has been developed to a high level of efficiency. Though exhibiting certain essential

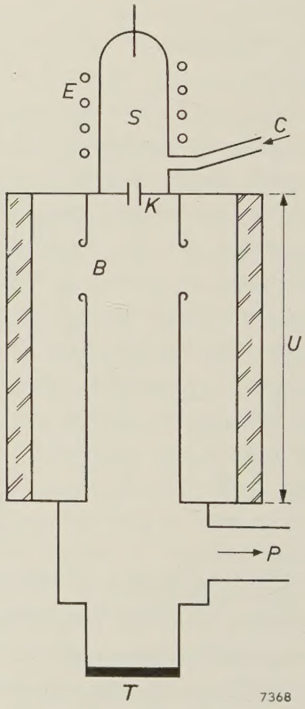

Fig. 1. Principle of a simple particle accelerator. Gas atoms are ionized in the discharge space S of an ion source (the source shown here is of the high-frequency type; E represents the RF coil). The ions leave the source via a small duct K and, in the evacuated cylindrical acceleration chamber B, they pass through a large difference of potential U; with the high energy thus acquired, they strike target T. I is a high-tension insulator. P is the tube through which the whole system is continuously evacuated; a stream of fresh gas is fed to the ion source via intake C. By choosing a suitable gas for ionization, and a suitable target material, neutron-yielding nuclear reactions can be caused to take place.

differences, our neutron tube shares many features with a particle accelerator and for that reason it will be as well to devote a little time to the principle of the latter (*fig. 1*). Gas molecules are converted into ions in an ion source S. Via K, a narrow cylindrical duct, some of the ions enter the evacuated cylindrical acceleration chamber B where they fall through a large potential difference U; having thus acquired a high kinetic energy, they strike an electrode of suitable material, the target T (usually earthed), with which they enter into a neutron-yielding nuclear reaction. The ancillary apparatus includes, apart from a high-tension generator, various devices omitted from fig. 1 for the sake of simplicity — namely, an HF generator for the ion source, with power supply unit, a complete vacuum system embodying backing and high-vacuum pumps and cold traps, and a gas storage and supply system, with a sensitive control valve, for the ion source. Though free of the drawbacks of the type containing radioactive substances, accelerator-type neutron sources are generally very large and expensive installations that often have to be housed in a separate building [3]) (see also the photograph on page 341 of this issue).

In recent years there have been various attempts to build compact and, if possible, transportable versions of these accelerator-type neutron-generating equipments. On the basis of reaction (3) above, these compact generators have become a practical possibility mainly in consequence of the availability of tritium in adequate quantities. Nowadays this isotope of hydrogen can be produced from lithium in nuclear reactors, using the reaction $^6Li(n,\alpha)^3H$. Reaction (3) shows that with tritium as the target nucleus, a fairly high neutron yield is obtained even when the voltage accelerating the bombarding deuterons (i.e. deuterium ions) is relatively low (60 kV for example). The effective cross-section for the D-T reaction exhibits a peak at the unusually low energy of 107 keV. In virtue of all this it has been possible to build neutron generators which, while still rather complicated in design, and necessarily including a complete vacuum system, can be mounted on trolleys and so moved from place to place.

While enumerating the various types of neutron source and generator we must not neglect to mention that nuclear reactors are nowadays the biggest-scale producers of neutrons [4]). The reaction taking place in these is of a different nature from those of reactions (1) - (3), namely nuclear *fission*. As a result of bombardment with neutrons, and also to some extent as a result of slow neutron capture, certain nuclei (^{233}U, ^{235}U and ^{239}Pu) can be caused to split and to release further neutrons, a series of these neutron-yielding reactions thus being initiated. A small proportion of the neutrons can be extracted via a duct in the shield of the reactor without prejudice to the continuity of the process. For many applications requiring a high neutron flux, a better source than a nuclear reactor is hardly likely to be found. Yet such big, complicated and costly installations are of course available only in a limited number; in practice, therefore, their usefulness as neutron sources is limited. Also a transportable neutron source in the form of a nuclear reactor is probably not a practical possibility.

There is a third category of neutron-yielding nuclear reactions which should be mentioned here for the sake of completeness; "photonuclear" reactions occur when nuclei are exposed to high-energy γ-radiation. In neutron sources working on this principle, the γ-radiation is either obtained from a radioactive substance — this type has the same disadvantages as the radioactive sources discussed above — or produced in a large particle accelerator with the aforementioned drawbacks of complicated design and high cost.

It may be noted in passing that scientific resources are currently being lavished on attempts to realize a further theoretical possibility, namely that of using the thermal energy of gases and plasmas at extremely high temperatures in order to induce nuclear *fusion*. A "fusion reactor", if it were ever built, would be a particularly rich source of fast neutrons.

A big advance in the direction of a compact, straightforward, monoenergetic neutron source was made with the development of an accelerator-type neutron generator in the form of a sealed tube; the need for a pumping arrangement and a continuous supply of gas for the ion source thus being eliminated. The Philips neutron tube [5]), based on this principle and under development since 1955, is shown in *fig. 2*; its general construction is shown in *fig. 3*. The tube bears a certain family resemblance to an X-ray tube; it has been possible in virtue of this to make use of accumulated experience in X-ray tube design, particularly in the matter of high-tension insulation and the prevention of arcing. However, in regard to the principle on which it works, the neutron tube is a direct descendant of the conventional particle accelerator (fig. 1). It accordingly displays the same essential structural features — an ion source, accelerating electrodes and a target that, bombarded by the accelerated ions, emits neutrons in virtue of the D-T reaction (3). The yield is in excess of 10^8 neutrons/sec.

---

[3]) See for example A. C. van Dorsten and J. H. Spaa, A high output D-D neutron generator for biological research, Nucl. Instr. **1**, 259-267, 1957, or Philips tech. Rev. **17**, 109-111, 1955/56.

[4]) A reference to the use of a nuclear reactor as a neutron source may be found in J. Goedkoop, Neutron diffraction, Philips tech. Rev. **23**, 69-82, 1961/62 (No. 3).

[5]) In the meantime neutron generator tubes have been described by other authors: J. D. Gow and H. C. Pollock, Rev. sci. Instr. **31**, 235-240, 1960. P. O. Hawkins and R. W. Sutton, Rev. sci. Instr. **31**, 241-248, 1960. A. H. Frentrop and H. Sherman, Nucleonics **18**, No. 12, 72-74, 1960. B. J. Carr, Nucleonics **18**, No. 12, 75-76, 1960.

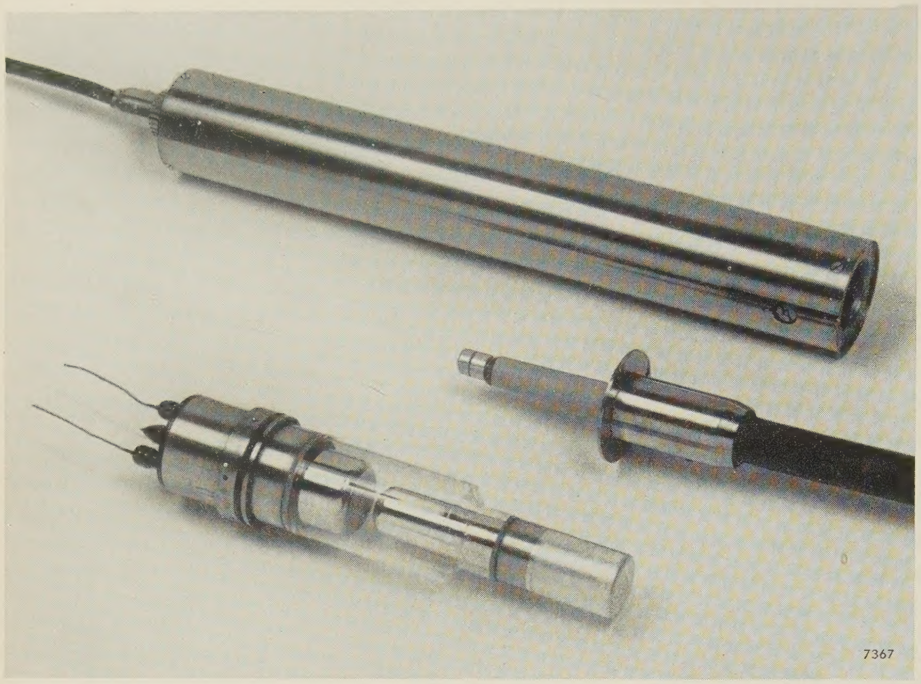

Fig. 2. The Philips neutron tube (at bottom in photo). The left-hand end of the tube, containing the ion source and a hydrogen pressure regulator, is at earth potential. High tension is applied to the right-hand end, via a HT cable and plug (centre). The tube as delivered (top) is enclosed in a metal cylinder with an outer diameter of 7 cm. This cylindrical sheath, which is earthed, affords mechanical protection and holds the HT insulation in place around the tube; it does not present any appreciable obstacle to the neutrons issuing from the target. These are expelled in all directions, but normal practice is to use only those with directions perpendicular to the tube axis.

One minor difference from a particle accelerator is that the high tension is applied to the target and the ion source is earthed; this arrangement offers certain operational advantages.

In the next section we shall deal with three main problems presented by the design of the neutron tube and explain how we have solved them.

The neutron tube: fundamental problems and their solution

A characteristic of accelerator-type neutron sources of the type shown in fig. 1 is that the particles to be accelerated are produced in a chamber in which a relatively high pressure prevails (of the

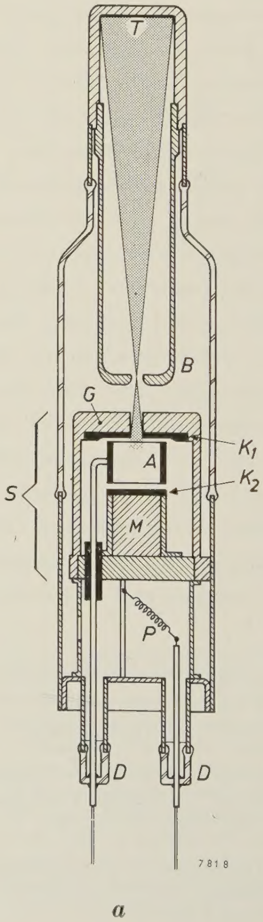

a

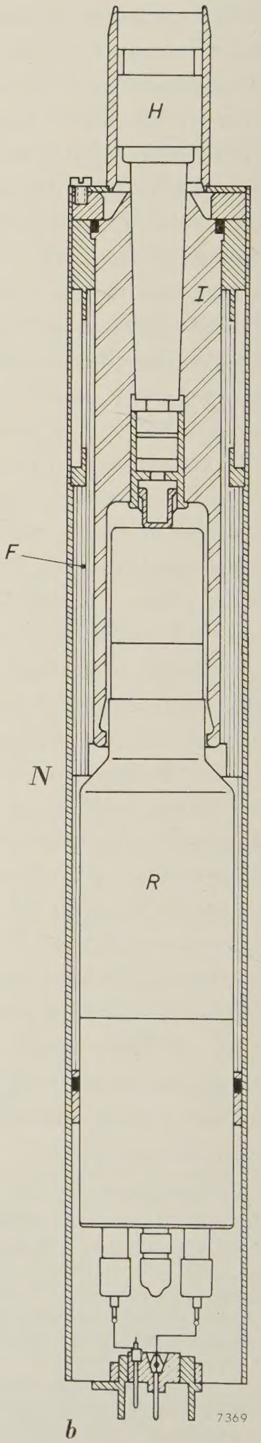

b

Fig. 3. *a*) Constructional details of the Philips neutron tube. *S* Penning ion source, at earth potential, also acting as one electrode of the accelerating stage. *B* high-tension electrode, to which an accelerating voltage of 125 kV is applied. *D* feed-through insulators for supply voltages to ion source (2 to 3 kV) and hydrogen pressure regulator *P* (0 to 2 V). *G* soft iron walls of ion source chamber. *M* permanent magnet. K_1, K_2 are the disc cathodes and *A* the cylindrical anode of the Penning ion source. *T* target. The ion beam is shaded; its shape is determined by the properties of the electron-optical lens formed by *G* and *B*.
b) Section through the neutron tube *R* enclosed in its earthed metal sheath *N*. *I* Araldite insulator. *F* oil-impregnated insutaing foil. *H* plug of HT cable.

order of 10^{-2} torr) whereas acceleration takes place in a space under relatively low pressure (of the order of 10^{-5} torr). The pressure difference between ion source and acceleration space is maintained by continuously feeding gas into the former (via inlet C) and continuously evacuating the latter by means of a high-vacuum pump. Now, in a *sealed* neutron tube this continuous gas flow must be dispensed with, and so in consequence must the pressure difference between the ion source and the accelerating space.

Thus the first problem involved by a sealed neutron tube is that of designing an ion source and an accelerating system that will work at the same gas pressure. If an intermediate pressure value is decided on, then the gas discharge in the ion source must sustain itself at a relatively low pressure and at a voltage that is not unduly high; the implication for the accelerating stage is that *no* discharge or flashover must take place between the accelerating electrodes despite the high voltages these are required to carry, and despite the relatively high pressure prevailing.

A second problem, likewise connected with the absence of a stream of gas through the tube, is that of gas clean-up as a result of the discharge. In a sealed tube this effect involves a rapid fall-off in pressure. Some expedient must therefore be found for keeping the gas pressure during operation constant throughout its useful life.

A third problem inherent in a sealed neutron tube is that of target life. Tritium targets of the type commonly used hitherto (in tubes exploiting the D-T reaction) have only a limited life, shorter than is generally desirable in a sealed tube. Obviously there can be no question, in such a tube, of replacing the target at intervals, as is possible in pumped neutron generators.

The ion source

The first of the problems referred to above — that of finding an ion source that will work at low pressures — can be solved by recourse to a device known for twenty-five years. It was precisely the fact that the Penning ion source could function at a relatively low pressure that led its inventor to design a sealed neutron tube ²). As in other ion sources, the ions are produced in a gas discharge, i.e. mainly by the impact of electrons. For this it is necessary that the mean free path of the electrons should be smaller than the distance available for them to travel through. Now, in other ion sources this distance is of the same order as the dimensions of the discharge chamber, and consequently the mean free path must be small and, generally speaking, the pressure must be in excess of 10^{-2} torr; the Penning ion source is so designed that the average distance travelled by the electrons is many hundred times greater than the electrode separation. This is achieved by using a special electrode layout and introducing a magnetic field. In these circumstances, then, there is still plenty of chance of ion formation by electrons with a large mean free path; it is therefore possible for the source to work at a lower pressure (10^{-3} to 10^{-4} torr).

A further virtue of the Penning ion source is its simplicity. No heated filamentary cathode is used: the discharge is sustained by electrons released from cathode plates by ion impact and by the photo-electric effect; accordingly, only one DC supply of about 2 kV is required for the ion source.

Fig. 4 is a schematic cross-section through the Penning type ion source incorporated in our neutron tube ¹). A cylindrical anode A lies between two disc-shaped cathodes K_1 and K_2. A direct voltage of 2 to 3 kV is applied between the anode and the cathodes. In the resulting discharge, electrons oscillate between the cathodes many times before finally striking the anode, being forced into helical paths by the magnetic field. The ions created by collisions between electrons and gas atoms move towards the cathodes. Some are able to quit the ion source chamber through an opening in cathode K_1. The mag-

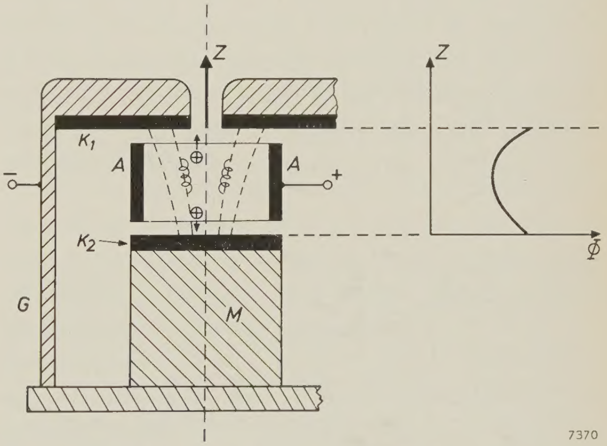

Fig. 4. Schematic cross-section of the ion source incorporated in the Philips neutron tube. G walls of ion source chamber. A is the anode, K_1 and K_2 the cathodes of the Penning electrode system. M permanent magnet. The broken lines represent magnetic lines of force; the magnetic circuit is completed by the soft iron walls G of the ion source chamber. Z direction of ion beam leaving the chamber. Φ is the electrical potential as a function of the distance z alang the axis of the tube; the electrons sustaining the discharge swing back and forth in the resulting potential well between the cathodes (see diagram) and are forced by the magnetic field into helical paths. The distance travelled by the electrons is thus many times greater than the geometrical electrode separation. It is for this reason that the discharge can sustain itself at gas pressures as low as 10^{-3} torr.

netic field is brought about by a small permanent magnet *M* which is accommodated inside the chamber. The walls of the chamber *G* are of soft iron, and so serve to complete the magnetic circuit and to screen the neighbouring acceleration space from the magnetic field in the ion source. This is important from the standpoint of freedom from high-voltage breakdown in the acceleration space, since a magnetic field increases the chance of ionization by electrons and so lowers the striking voltage for a self-sustaining discharge. This fact is exploited in the ion source itself, but just the opposite desiderata are relevant to the acceleration space.

The Penning ion source has a certain drawback in that it mainly supplies singly-charged molecular ions (H_2^+ with hydrogen as filler gas, D_2^+ with deuterium) in the range of pressures of interest. This we discovered at the outset, in 1956, when the ion beam was submitted to mass-spectrometric analysis in our Research Laboratories (*fig.* 5). For a given discharge current, the number of atoms in a beam of singly-ionized diatomic molecules is twice as large as that in a beam of monatomic ions. Moreover, each of the two atoms in the ionized molecule acquires only half of the total energy, so that in a neutron tube operated at 125 kV, only 62.5 keV of primary energy is available for the nuclear reaction. Since in this range of energies the probability of the reaction taking place diminishes sharply with decreasing voltage, the final result is that the neutron yield is lower than it would be with a beam of monatomic ions. This drawback of the Penning ion source has been accepted in view of the far greater importance attached to its advantages — long life, robustness, and simplicity of construction and operation.

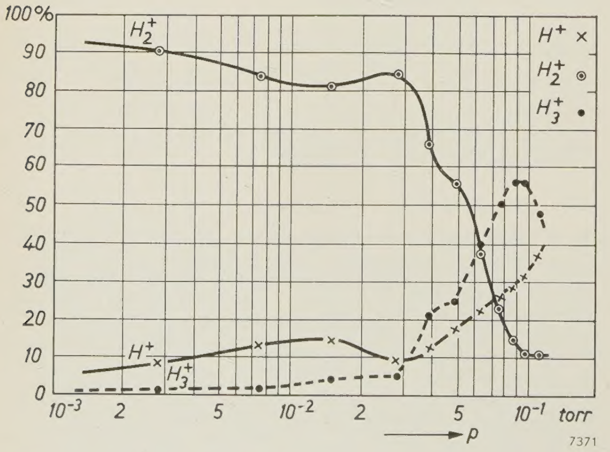

Fig. 5. Composition of the beam of hydrogen ions produced by a Penning ion source, as a function of pressure. In the range between 10^{-3} and 3×10^{-2} torr the beam mainly consists of molecular (H_2^+) ions.

Arrangements for feeding in the direct-voltage supply are greatly simplified by the fact that the ion source is at earth potential.

The 125-kV acceleration stage

Conventional accelerators working in conjunction with a pump operate at pressures lower than 10^{-4} torr, and acceleration generally takes place in several stages. Preliminary experiments [1]) revealed that a 200 kV acceleration system, to operate at pressures up to 2×10^{-2} torr, could be designed as a single stage. The electrode separation in these experiments was about 1 cm. Accordingly, no design difficulties would be involved by a neutron tube operating at a pressure of 10^{-3} torr and an accelerating voltage of 125 kV. It would, however, be necessary to give the electrodes a high polish, since otherwise there would be a risk of field emission from the negative electrode. Accelerating electrodes for the neutron tube described here are made of chrome steel which, as experience with X-ray tubes has shown, exhibits very little liability to field emission.

As will be clear from the sketches in fig. 3, accelerating electrode *B* has an opening through which the ion beam enters the field-free space inside the electrode. The beam is conical in shape, its apex angle being determined by the properties of the electron-optical lens formed by the ion source and accelerating electrode. *Fig. 6* is a photograph of the ion beam in an experimental tube. In the final version of the neutron tube, as developed on the basis of findings from these experiments, the target is set up at a distance from the ion source such that its whole surface is just covered by the ion beam (fig. 3*a*). This results in efficient loading of the target and hence in a better neutron yield. If the target were placed only 1 cm in front of the ion source, the narrow ion beam would strike only a restricted area of the target surface, with undesirable local overheating as a result. The tubular form of the accelerating electrode has the further advantage of allowing it to catch most of the secondary electrons leaving the target, thereby preventing their acceleration back into the ion source. If allowed to travel through the whole acceleration space the secondary electrons would lower the breakdown voltage in consequence of the ionization they would cause; they would also be responsible for unnecessary heating of the walls of the ion source, and the unwanted heat would be conveyed by conduction to other parts of the tube; finally, the secondary electrons would generate X-radiation of the bremsstrahlung type, which would be undesirable in many applications of the neutron tube.

The hydrogen pressure regulator

The second problem, that of regulating and stabilizing the gas pressure inside the tube, calls for a device whereby additional filler gas can be supplied and, if necessary, withdrawn again.

If in the course of the manufacturing process the tube were filled with gas at the desired pressure and then sealed, this pressure would be liable to fall off rapidly when the tube was taken into operation, in consequence of gas clean-up in the discharge. This loss is mainly a result of gas ions being shot into the electrodes and the walls of the discharge chamber.

For replenishing the gas supply to the ion source, conventional accelerator-type neutron generators embody a valve, e.g. a small electrically-heated tube of palladium or nickel, through which hydrogen isotopes readily diffuse at higher temperatures; such devices are unsuitable for a sealed tube because they can only be used to bring about a *rise* in pressure. It would accordingly be impossible — by this means alone — to compensate the spontaneous pressure rises that occur, for example, if previously occluded filler gas is released in consequence of normal heating of the tube in operation.

An efficient hydrogen pressure regulating device (hydrogen replenisher) can be based on the fact that certain metals absorb hydrogen exothermically. Amongst these are zirconium and titanium, which are able to take up large quantities of hydrogen or hydrogen isotopes, evolving heat at the same time, and release them when heat is applied from the outside. Care must however be taken to ensure that the surface of the metal offers no obstruction to the passage of the gas, i.e. that it is physically and chemically clean.

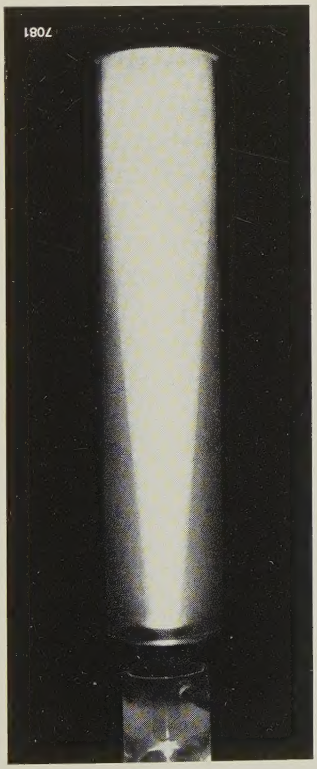

Fig. 6. Photograph of the ion beam in an experimental version of the neutron tube, which was expressly built up mainly of glass in order that the beam could be studied.

If a metal-hydrogen system of this kind is placed in a vacuum-tight vessel, the gas pressure will attain an equilibrium value p which is related to the absolute temperature T by the Clausius-Clapeyron formula:

$$\ln p = -\frac{\Delta H}{RT} + C$$

where R is the gas constant, ΔH is the heat of reaction, and C is a constant of integration. Thus the equilibrium pressure increases with temperature and, given a metal-hydrogen system whose temperature can be varied, we shall have, in principle, a device for regulating the pressure of the hydrogen. Generally speaking, an increase in the number of atoms per metal atom, such as may be occasioned by release of gas from other parts of the tube, will result in a rise in pressure that has to be compensated by lowering the temperature of the system. However, there is a range within which the equilibrium pressure is *not* dependent on the ratio between the number of hydrogen atoms and the number of metal atoms present. This useful fact can be explained in terms of a phase transformation, and in our tube advantage is taken of it to keep the gas pressure constant.

In its simplest form, the pressure regulator consists of a zirconium wire wound for the sake of mechanical stability around a tungsten wire [6]), the whole being built into the neutron tube (P in fig. 3). The zirconium wire is charged with gas before the tube is sealed, and thereafter its temperature can be conveniently and reproducibly adjusted by passing an electric current through it. In operation, then, the pressure inside the tube can be adjusted to the desired value by altering the voltage across the ends of the wire (see *fig.* 7).

Like the ion source, the pressure regulator is at earth potential, so that no difficulty is involved by feed-in arrangements for the heater current.

---

[6]) K. Nienhuis, Hydrogen-filled electric discharge devices, U.S. Patent 2 766 397. This pressure regulator was first used in hydrogen thyratrons, and allowed their useful life to be increased to several thousands of hours. See also Philips tech. Rev. **20**, 102, 1958/59 (fig. 2).

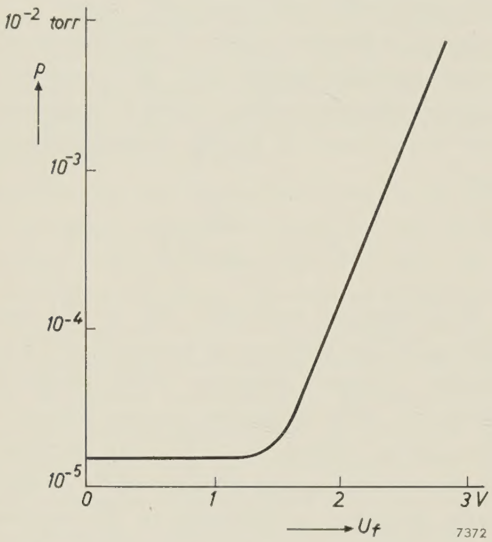

Fig. 7. Pressure p in the neutron tube, as a function of the voltage U_f across the filament of the hydrogen pressure regulator.

A drawback of this design is that the rate at which hydrogen is absorbed is rather slow, particularly at low pressures, in consequence of the inevitable poisoning of the zirconium wire, the superficial area of which is comparatively small. To get a system with a faster response it is necessary to increase the area available for absorbing hydrogen. This has been done by employing the absorbing metal in the form of an extremely fine powder deposited by evaporation on the surface of a different metal [7]). Instead of zirconium, titanium is used as absorbing metal. The pressure regulator in our neutron tube consists of a cylinder made of thin nickel sheet with a heater wire mounted inside it. Around the heater is wound a titanium wire which is evaporated, not in vacuum, but in argon at a pressure of about 10 torr, in consequence of which it deposits itself on the inside of the cylinder as a kind of soot. The deposit is composed of spherical grains which are about 100 Å in diameter, and therefore much smaller than could ever be obtained by mechanical crushing of the titanium. This fine powder will absorb large quantities of hydrogen and its isotopes very quickly [8]), and quickly release the gas when heated. In operation, the wire originally used for evaporating the titanium serves as a heating element for the pressure regulator. For example, to obtain a deuterium pressure of 10^{-3} torr inside the tube, the temperature of the titanium deuteride must be maintained at about 260 °C.

The target

Only one main component of the neutron tube remains to be dealt with, namely the target. The output and useful life of the tube are mainly governed by the target quality. Our neutron tube exploits the D-T reaction, of which mention has several times been made in the foregoing and which was numbered (3) above; under the primary energy conditions designed into the tube, this reaction yields neutrons with an energy of about 14 MeV at an angle of 90° to the primary beam. To bring about the D-T reaction, deuterons must be shot into a *tritium* target, and since tritium is a gas, some way must be found of occluding it or anchoring it to a solid body. Tritium targets suitable for conventional accelerator-type neutron generators are commercially available, and consist for example of a metal disc 0.2 mm thick on to which has been evaporated a film of zirconium or titanium about 1 μm thick saturated with tritium. Our experiments showed that titanium-coated targets had a higher neutron yield than zirconium-coated ones, and were better able to stand up to high temperatures. We found that they could be freed from impurities by degassing at temperatures as high as 200 °C and brazed on to the target support without any loss of tritium. However, these commercial targets have two drawbacks that render them less suitable for use in a sealed neutron tube: firstly degassing cannot be done at temperatures above 200 °C, and secondly, experience with conventional neutron generators indicates that the targets may have a life of only a few hundred hours. Ways and means were therefore sought of circumventing this limitation on the life of the tube [1]).

One way out of the difficulty was offered by the "drive-in" types of self-replenishing target that have several times been described in the literature [9]). If a plate of metal such as gold is bombarded with deuterons with energies of several hundreds of keV, the particles penetrate the metal and spread through it by diffusion. In this way a deuterium target is gradually formed; deuterons subsequently striking the plate enter into the D-D reaction, producing neutrons. In an experiment of this kind, then, it is very soon found that neutrons are being emitted, and the rate of emission increases as time goes on. Generally, after a certain lapse of time, the yield attains a saturation value. The reason is that, by this time, a certain proportion of the deuterons shot into the metal are diffusing back to the surface and out of the plate. A steady state of saturation is attained when the deuterons diffuse out of the target at the same rate as they are shot into it.

---

[7]) O. Reifenschweiler, Ein Druckregler für Wasserstoffisotope mit grosser Einstellgeschwindigkeit des Gleichgewichtsdrucks, Phys. Verh. (Mosbach) Verbandsausgabe, 1961, 181 (No. 9).

[8]) For many purposes the gaseous radioactive hydrogen isotope tritium can be handled more conveniently if it is absorbed in this way and the titanium powder is prepared as a suspension. See. O. Reifenschweiler, A suitable tritium carrier for gas discharge tubes, Proc. 2nd United Nations Intern. Conf. Peaceful Uses Atomic Energy **19**, 360-362, Sept. 1958, Geneva.

[9]) Self-replenishing targets exploiting the D-D reaction were first investigated thoroughly by K. Fiebiger, Die Bildung von „Selbsttargets" für die Kernreaktion D(d,n)^{3}He und ihr Zusammenhang mit dem Problem der Wasserstoffdiffusion in Metallen, Z. angew. Physik **9**, 213-223, 1957.

The proportion of deuterons "used up" by nuclear reactions is extremely small, so small that it has no effect on the constitution of a self-replenishing target. Fiebiger's experiments [9]) indicated that the highest saturation concentration of deuterons and the greatest neutron yield was obtainable with a gold self-replenishing target.

So far we have dealt only with the self-replenishing target for the D-D reaction. One exploiting the D-T reaction can be produced by filling the neutron tube with a mixture of tritium and deuterium and using it to bombard the target. As a result, tritium as well as deuterium penetrates the target material, and enters into reaction with the incident deuterons. True, it also happens under these circumstances that deuterium and tritium ions strike deuterium atoms and that tritium ions strike tritium atoms, in consequence of which the neutron yield is only a third of that available when a pure tritium target is bombarded with deuterons. Measurements and approximate calculations have shown that, of the above competing reactions, only the D-T and T-D reactions — which naturally yield neutrons of the same energy — make any appreciable contribution to the output of the tube.

The reasoning underlying the above statements is as follows. Let us assume that, in a tube filled with deuterium and tritium in equal proportions, the ion beam and the gas absorbed into the target are also 1:1 mixtures of the two isotopes. The chances of a D-T, a T-D, a D-D and a T-T impact are in each case 25% of the probability that a D-T impact will take place in a tube with a pure tritium target and a beam composed exclusively of deuterons, other conditions (beam current, gas content of target etc.) being the same. The output from a tube of the latter kind may amount to 5×10^8 neutrons/sec; if this is regarded as a 100% yield, then the yield of 14-MeV neutrons from the D-T reaction in the tube filled with a gas mixture will only be 25%.

In regard to the contribution of the T-D reaction to the neutron yield of the tube, it must be remembered that the tritium ion has a mass 50% greater than that of a deuteron; consequently, the kinetic energy of the tritium ions in the beam, measured in relation to the centre of gravity of the system formed by the two reacting particles, is only two-thirds that of deuterons accelerated through the same potential difference.

The energy available for a nuclear reaction is equal to the kinetic energy of the reacting particles due to their motion relative to their common centre of gravity; their movement relative to an outside frame of reference is irrelevant. Consequently 60-keV tritium ions are only equivalent to 40-keV deuterons. On account of the smaller effective cross-section of the D-T reaction at 40 keV, its neutron yield at this primary energy is only a quarter of what it would be at a primary energy of 60 keV. This latter, as we have already established, would be 25% of the yield from a tritium-target deuteron-beam tube. The actual yield of 14 MeV neutrons from the T-D reaction is therefore about 6%.

The contribution of the D-D reaction can be worked out from the measured yield from tubes filled with pure deuterium. These have been found, under the same operating conditions, to produce 5×10^5 neutrons/sec. In the mixture-filled tube only a quarter of the reactions are D-D reactions. Accordingly, these will contribute 1.25×10^5 neutrons (of 2.5 MeV) per second, which represents less than 0.1% of the overall yield from a "pure" D-T tube.

Finally, in regard to impacts of tritium ions on tritium atoms, the chance of a nuclear reaction resulting from these is so slight at the accelerating voltages employed that it can be neglected altogether.

On adding the above contributions together we arrive at a figure of about 31%. Accordingly, a neutron tube filled with a deuterium-tritium mixture has a yield about one-third of that from a tube with a pure tritium target and a beam composed exclusively of deuterons. Of this overall yield, the D-T reaction is responsible for four-fifths and the T-D reaction for one-fifth, both these reactions yielding 14-MeV neutrons. The D-D reaction, yielding 2.5-MeV neutrons, contributes less than 0.1% to the tube output.

The above considerations still fail to take full account of actual conditions in the tube, since the particles accelerated are mainly molecular ions, not monatomic ones. During absorption into and desorption from the hydrogen pressure regulator, the formation of D-T molecules may occur, so that we really have three kinds of molecule to deal with; in the ideal case these would be present in the proportions 1:2:1. However, the result of a more elaborate study taking account of all such factors would not differ appreciably from the figure just arrived at.

The use of drive-in targets removes a limitation on the tube life, which ceases to be dependent on that of the target. A further advantage is that the temperature at which the tube can be degassed and evacuated ceases to be governed by the thermal properties of the target, since this is not charged with gas until after the tube has been sealed. Still, as has already been shown, the usual type of drive-in target has a smaller neutron yield than the targets commercially available, and for that reason we cast about for a better type. As will now be explained, we have succeeded in designing drive-in targets that have an appreciably higher neutron yield.

Gold, which Fiebiger's experiments indicated was the best material for drive-in targets, does not naturally occlude hydrogen isotopes. In fact, in the target experiments, it is *forced* to absorb the isotopes, these being shot into it at high velocity;

thereafter, they distribute themselves through the metal by diffusion. The diffusion coefficient of hydrogen isotopes in gold is small but, of course, increases with temperature. Consequently it is only in a superficial layer of the target heated by ion bombardment (the thickness of which corresponds to the maximum range of the ions penetrating the surface) that distribution of the hydrogen isotopes is at all efficient, by reason of the rather higher diffusion coefficient of this heated layer. Hence the highest concentration obtainable within the layer penetrated by incident ions — the only part of the target where nuclear reactions are likely to take place — is governed by the rate at which the ions are diffusing out of the layer via the target surface; diffusion into the depth of the target, *away* from the surface, can be neglected. This theory of Fiebiger's was confirmed by his experiments on gold targets [9]). The above is outlined in visual terms in *fig. 8a.*

Unlike gold, the metals zirconium and titanium are able to go on absorbing hydrogen isotopes exothermically right up to the point of hydride formation, a property exploited in the pressure regulator. This means that throughout the charging process, i.e. until the target has become saturated, there is a potential barrier at its surface, hindering the escape of hydrogen isotopes from the metal. It is therefore easier to achieve and maintain a high concentration of hydrogen isotopes in titanium or zirconium than in gold, provided only that some means can be found of preventing too many of the hydrogen atoms from escaping at the *other* side, beyond the limit of the reaction zone, as they are liable to do in consequence of the high diffusion coefficients of zirconium and titanium. This is made clear in fig. 8*b*. It is obvious that in Fiebiger's experiments on drive-in targets, zirconium and titanium only gave poorer neutron yields than gold because the ions were escaping at the back door, so to speak.

Diffusion out of the reaction zone can be prevented by using the target metal in the form of a thin layer applied to a base with a low diffusion coefficient for hydrogen. The thickness of the layer must more or less correspond to the range of penetration of the

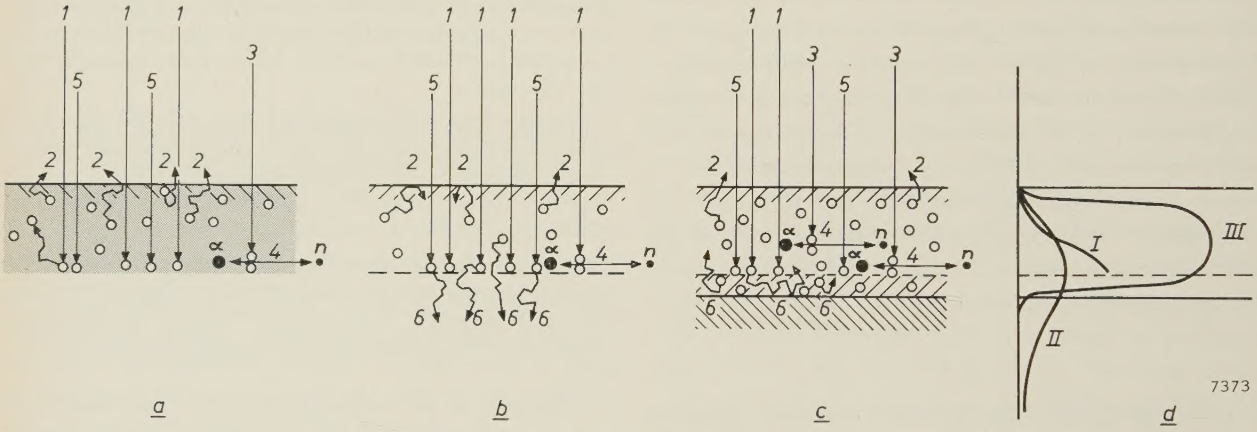

Fig. 8. The diagrams represent, schematically, various types of drive-in targets exploiting the D-D reaction.
a) Fiebiger's gold target [9]). Gold is a non-occluder of hydrogen isotopes: it does however absorb deuterium when bombarded with deuterons (*1*) of sufficient energy to effect penetration to some depth. In a thin layer of the target (grey area in the diagram) the deuteron concentration gradually attains a steady state as the nett result of a number of processes — penetration of the deuterons, their diffusion through the metal (only at high temperature), heating of the metal by the deuteron bombardment, and escape of the particles by diffusion out of the target (*2*). Deuterons present in the target may enter into neutron-yielding nuclear reactions (*4*) with newly arriving deuterons (*3*) or, alternatively, these latter may merely contribute to maintaining the concentration in the target (*5*). Curve *I* in diagram *d* shows the presumed concentration distribution of deuterium in a saturated drive-in target of gold [9]).
b) Solid titanium target. The numerals *1* to *5* have the same significance as in *a*. Unlike gold, titanium is an exothermic absorber of hydrogen isotopes, absorbing deuterium very readily up to the point of TiD_2 formation; a high saturation concentration ought therefore to be attainable in a titanium target. However, the incident deuterons cannot build up this high concentration because of the high diffusion coefficient of hydrogen isotopes in titanium even at room temperature. In consequence of this most of the deuterons diffuse further into the metal (*6*), out of the reaction zone. (The particles have to overcome a potential barrier before emerging from the target surface (*2*) and this effect is therefore unimportant.) Curve *II* in diagram *d* shows the presumed concentration distribution of deuterium in a titanium target; the neutron yield from such a target is accordingly smaller than in case *a*.
c) This diagram represents the backed titanium-film drive-in target employed in the neutron tube [1]). The thickness of the film is rather greater than the maximum range of the incident ions (*1*) in titanium and the backing metal is one that has a low diffusion coefficient for hydrogen. It is impossible for the particles to diffuse further into the depth of this target (*6*) and consequently the concentration of deuterons obtainable in the titanium film is very high. Curve *III* of diagram *d* shows the presumed distribution of deuterium densities. The neutron yield is three times as great as in case *a*.

Diagrams *a*, *b* and *c* are of course applicable to the D-T reaction as well as to the D-D reaction. In fact only a proportion of the small circles are to be regarded as deuterons; the others represent tritons. In addition to neutrons, α-particles are produced as a result of the D-T reaction (as shown); in the D-D reaction, however, ^{3}He nuclei are produced instead of the α-particles.

ions. On bombardment, the layer becomes charged up to saturation in a comparatively short time (about 15 hours at a beam current of 100 μA); the saturation concentration of hydrogen isotope is high (see fig. 8*c*). The present neutron tube is equipped with a target of this kind, consisting of an approximately 1 μm film of titanium evaporated on to a silver base. For an acceleration voltage of 125 kV and an ion current of 100 μA, a yield of over 10^8 neutrons/sec is obtained. Measured yields from the best of these targets have attained the figure of 2.4×10^8 neutrons/sec.

Apart from providing a roughly three times higher neutron yield, the titanium-film target has the advantage over the gold drive-in target of being better able to stand up to elevated temperatures, remaining stable up to 200 °C. Fiebiger found that the neutron yield from gold targets fell off steeply above 120 °C.

The neutron tube in operation

The necessary ancillary equipment includes a high tension supply (e.g. a Greinacher cascade generator) supplying 125 kV AC at currents ranging from 100 to 200 μA, and a power unit supplying 2 to 3 kV DC at 0.3 to 1.0 mA for the ion source, and 0 to 2 V AC at currents up to 5 A for the hydrogen pressure regulator (*fig. 9*). The current through the neutron tube is measured with a microammeter inserted in the HT lead, for example. Of course, part of this current is due to electrons liberated from the target and accelerated in the reverse direction, back to the ion source. The true ion current can be determined by calorimetric methods. An alternative method is to measure the X-radiation generated by the backward-accelerated electrons. Measurements using both methods revealed that ions are responsible for about 80% of the tube current.

The neutron yield can be measured with any kind of radiation detector responsive to neutrons; some detectors will require preliminary calibration. We have carried out an exact measurement by an activation method in which calibration is not necessary. The reaction ^{63}Cu(n,2n)^{62}Cu was induced by neutrons from the tube in a copper disc set up in the vicinity of the tube target. The ^{62}Cu thus produced is a positron emitter with a half-life of about 10 minutes. Consequently only a limited amount of ^{62}Cu is formed, determined by the balance between the rates of formation and decay of the isotope. Having measured the β^+-activity of the irradiated target (with an end-window counter tube), and knowing the effective cross-section of the (n,2n) reaction with the ^{63}Cu, it is possible to work out the neutron yield of the tube. The activation method was checked by the method of associated particles: In the D-T reaction an α-particle is liberated at the same time as the neutron and is emitted in the opposite direction (see reaction (3) above). The number of α-particles produced, as registered by an end-window counter tube, for example, is the same as the number of neutrons striking and activating a copper disc set up opposite the counter, provided the geometry of the arrangement is exactly symmetrical. There was good agreement between our results from the two methods — calculation on the basis of the effective cross-section and measurement of the associated α-particle production.

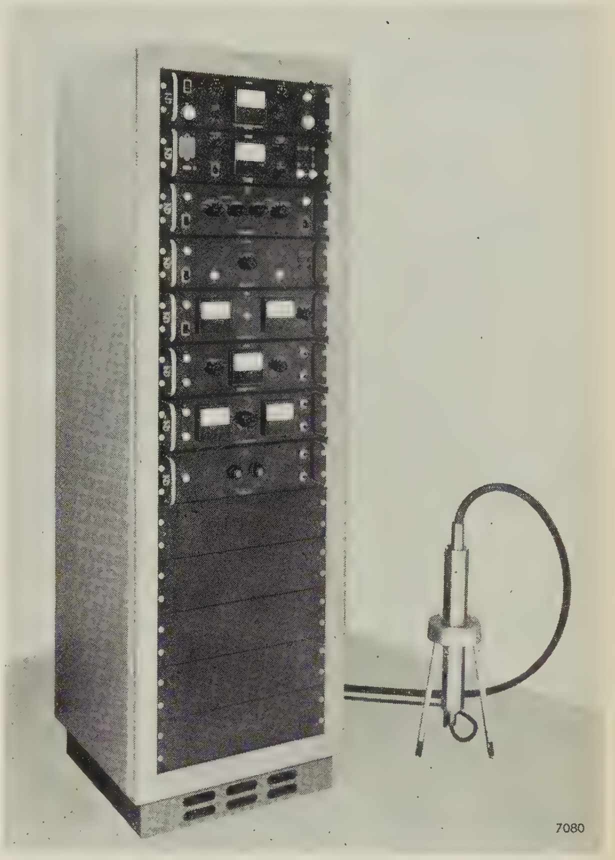

Fig. 9. The Philips neutron tube in its cylindrical metal sheath, complete with power supply. The rear of the lower part of the rack is occupied by the high-tension generator; there is room in front of this for five units for measuring and other purposes. Immediately above are the four units necessary to the operation of the neutron tube; the lowest is a power pack and the other three, taken in ascending order, contain control and monitoring circuits for the HT supply, the hydrogen pressure regulator and the ion source. Accommodated in the rack above these are the pulse generator necessary for pulsed operation of the tube (two units) and counter circuits embodying a count-rate meter, for measuring and checking the neutron flux (two units).

Further experiments were done to determine the neutron yield from a saturated Ti-film drive-in target as a function of accelerating voltage. In addition, neutron yields under various conditions were calculated from the effective cross-section of the D-T reaction and the atomic stopping power of titanium tritide, for different ion beam compositions and for two different targets, one with a tritium-titanium ratio of 1:1 and the other with a deuterium-tritium-titanium ratio of 1:1:2. The results are displayed in *fig. 10*. It will be noted that the measured curve lies very close to the relevant calculated one. At an accelerating voltage of 125 kV and an ion current of 100 μA — under which operating conditions the tube is very stable — a yield of more than 10^8 neutrons/sec is obtained. Fig. 10 also shows that the employment of a pure tritium target and a pure deuterium atmosphere would increase the neutron yield by a factor of 3; however, as has already been explained, the life of the tube would then be limited to a few hundred hours.

The drive-in target actually embodied in the tube has an almost unlimited life. Several tubes taken from the production line have been life-tested under the above conditions (accelerating voltage of 125 kV at ion currents of 100 or 200 μA, corresponding to neutron yields exceeding 10^8 and 2×10^8 neutrons/sec respectively) for periods exceeding 1000 hours; one tube has been run for 4000 hours. No fall-off in reliability of operation or in neutron yield could be detected either during or after these tests.

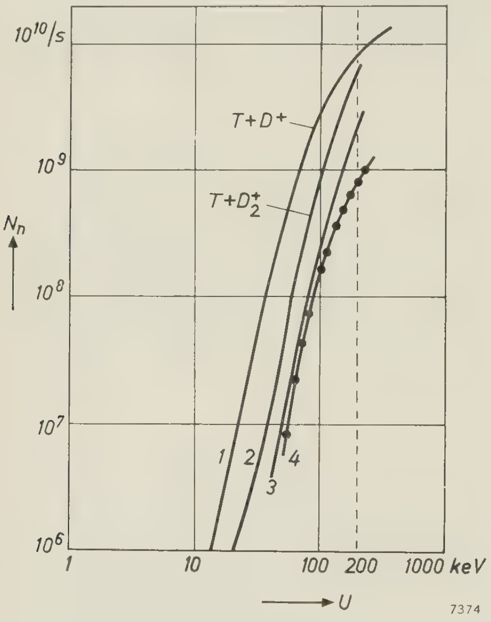

Fig. 10. The yield N_n in neutrons per second at a tube current of 100 μA, as a function of the accelerating voltage U. Curves *1*, *2* and *3* are theoretical, and curve *4* is experimental. Curve *1* has been plotted from calculated yields based on the effective cross-section of the D-T reaction and on the atomic stopping power of the titanium tritride in a target in which titanium and tritium are present in the ratio of 1:1. Furthermore, the ion beam has been assumed to be composed exclusively of monatomic D^+ ions (deuterons). Curve *2* relates to the case where the ion beam is mainly composed of molecular D_2^+ ions; neutron yields are only one-third of those obtained in the case to which curve *1* relates. Curve *3* shows calculated neutron yields in the case where the filler gas, and hence the ion beam, is a 1:1 mixture of deuterium and tritium (molecular ions) and the target is a titanium-film drive-in type, all other conditions remaining the same. These are the conditions appropriate to the final version of the neutron tube, and there is good agreement between this theoretical curve and curve *4*, which is a plot of values obtained from actual measurements.

The neutron yield can be adjusted to any desired value between zero and maximum by varying the accelerating voltage; an alternative method of controlling the tube output is by adjusting the gas pressure in the tube or the voltage across the ion source. It is also possible to stabilize the neutron yield; generally it suffices to keep the ion source current constant, and this can be done automatically by a feedback arrangement whereby this current controls the voltage across the hydrogen pressure regulator. About 10^{-3} torr has been found to be the most favourable gas pressure.

A pulsed neutron output is desirable in many applications of the tube; this can easily be effected by pulsing the ion source voltage. The minimum usable pulse duration is 5 μs. During a pulse, the neutron yield is about 10 times greater than it is under continuous operation; hence, if the pulse occupies 10% of the cycle (i.e. intervals 9 times the pulse length) the mean neutron output will be roughly the same as under continuous operation.

Applications of sealed-off neutron tubes

Finally, let us take a look at a few typical applications of neutron tubes. It must be made clear from the outset that these sources are *not* designed to produce the less common elementary particles that are the speciality of extremely large accelerators. The usefulness of the neutron tube described here lies rather in the fact that it is a particularly simple, convenient and comparatively cheap source of fast, monoenergetic neutrons, its main advantage over conventional accelerators being that it is readily transportable.

Fundamental research in nuclear physics, and particularly in neutron physics, immediately suggests itself as the most obvious field of application for neutron tubes in those cases where a yield 10^8 neutrons/sec is sufficient. The tubes are accordingly being used for investigating the elastic and inelastic scattering of fast neutrons, for studying slow neutron capture, for producing radioactive isotopes and investigating their properties, and for calibrating neutron spectrometers [10]), Wilson chambers, bubble chambers and nuclear emulsions.

---

[10]) L. J. de Vries and F. Udo, A fast pulse-shape discriminator with applications as a spectrometer and sensitive monitor for 1-30 MeV neutrons, Nucl. Instr. and Meth. **13**, 153-160, 1961 (No. 2).

A further broad field of application for neutron tubes arises out of the employment of the neutron in fields outside nuclear physics for the solution of both purely scientific and more immediately practical problems. For example, the tubes are convenient for producing small quantities of short-lived artificial radioactive isotopes on the spot. This facility is of value in chemical and biological research, and it is relevant to many of the problems with which engineers are confronted. It is particularly in connection with the production of *short-lived* isotopes that the advantages of the neutron tube become evident: normally a nuclear reactor is not available at the place where the isotopes are to be used, and the time required for transportation prohibits irradiation of the material in a reactor some distance away.

A further, related field of application is that of non-destructive analysis. Here a distinction must be made between two methods — activation analysis, and analysis by means of directly induced γ-emission. In activation analysis the sample is irradiated with fast or slow neutrons (cf. the method for measuring neutron yield described above). By investigating the resulting radioactivity of the sample — the half-life and/or the nature of the emitted radiation — the presence of various chemical elements can be determined quantitatively often with great accuracy. Almost all the elements can be identified in this way, though in some cases it may be necessary to undertake separation first or treat the sample afterwards, using ordinary chemical methods.

In the second method of non-destructive analysis, a γ-spectrometer is employed to investigate the γ-radiation generated during neutron bombardment of the sample by inelastic scattering of fast neutrons or by slow neutron capture (n,γ reaction). Analysis of the resulting γ-spectrum is thus analogous to X-ray spectrometry.

Both methods of analysis are highly suitable for geological investigations, the mobility of the neutron tube making it possible to assay mineral samples in the field. A typical application of great practical importance is the detection of petroleum in the vicinity of drillings ("oil-well logging"). Together with a suitable detector, the neutron source is lowered into the drill hole. In principle the activation method of analysis just described allows all geologically important elements to be identified. Methods based on the recording of γ-spectra seem to offer even better prospects, in view of the fact that γ-radiation can be detected more easily and more efficiently. A particularly useful aspect of these methods is the possibility of exploiting the delay between the γ-radiation generated by fast neutrons (i.e. due to inelastic scattering of the 14 MeV neutrons coming direct from the tube) and the γ-radiation generated by thermal neutrons (those slowed down by elastic scattering). This enables the elements carbon and oxygen to be differentiated more clearly from hydrogen, silicon and chlorine and, accordingly, salt or fresh water to be readily distinguished from mineral oil. Methods exploiting these time differences naturally call for a pulse-operated source of fast neutrons [11]).

The study of reactor materials represents another important field of application for neutron tubes with facilities for pulsed operation. Certain properties of reactor materials, important from the viewpoint of neutron physics, can be measured in subcritical rigs by injecting the materials with a brief, intense burst of neutrons. The tubes are also convenient for testing neutron-shielding materials.

Of no less importance is the employment of the neutron tube in education and technical training. The tube is simple to operate, it can be adjusted to supply any desired flux from zero to the maximum, and it should therefore represent an ideal neutron source for demonstrations in the lecture theatre and for practical work in the laboratory, opening up the interesting field of artificial radioactivity as well as that of neutron physics proper.

---

[11]) R. L. Caldwell and W. R. Mills Jr., Nucl. Instr. and Meth. **5**, 312, 1959; J. Tittman and W. B. Nelligan, Amer. Inst. Mining Engrs Casper (Wyoming) meeting, April 1959, Paper 1227 G; B. G. Erozolimskii, A. S. Shkol'nikov and A. I. Isakov, Atomic Energy (Moscow) **9**, 144, 1960.

Summary. After a brief review of current types of neutron sources, the authors describe a neutron source tube which is about the size of an X-ray tube, and is operated in a similar way. Supplied with a direct voltage of 125 kV, this tube is capable of generating neutrons with an energy of 14 MeV at rates exceeding 10^8 neutrons/sec. The neutrons arise out of a nuclear reaction between tritium and deuterium: $T(d,n)^4He$. The deuterons are produced in a Penning ion source and accelerated up to 125 keV in a single-stage accelerating system. They strike a target consisting of a 1 μm film of titanium which has been evaporated on to a silver base, and which contains tritium. The tube is filled with a deuterium-tritium mixture at a pressure of about 10^{-3} torr; consequently the target is bombarded with tritium ions as well as deuterium ions, and in this way its charge of tritium is kept at saturation more or less indefinitely. The life of the tube is not therefore limited by that of the target. The pressure inside the tube is adjusted by means of a built-in replenisher containing a large reserve of D-T mixture, so enabling gas clean-up to be compensated and removing a further restriction on the life of the tube. In life tests, a number of tubes have worked for periods exceeding 1000 hours (one for 4000 hours) without any fall-off in operating reliability or neutron yield. The yield from the tube can attain 10^9 neutrons/sec when it is pulse-operated (the shortest pulse duration is 5μs). In conclusion, some typical applications for this type of neutron tube are touched upon.

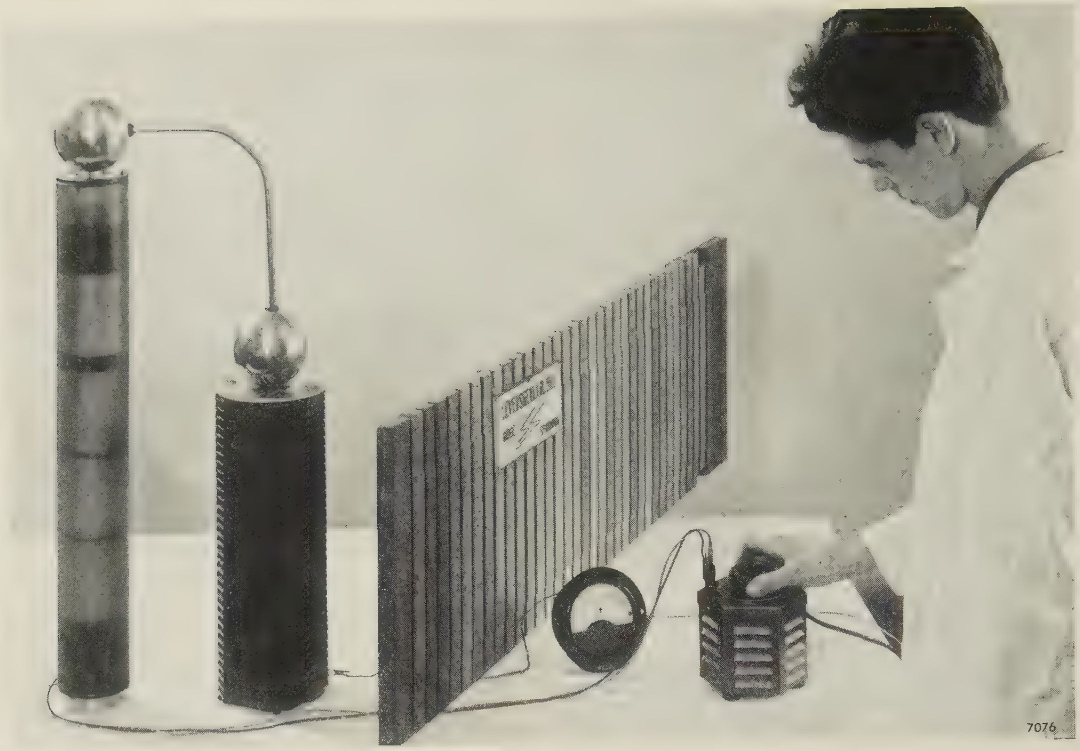

AN EXPERIMENTAL HIGH-TENSION GENERATOR OF VERY SMALL DIMENSIONS

by H. P. J. BREKOO *) and A. VERHOEFF **). 621.314.54

The high DC voltages needed e.g. in nuclear physics for particle accelerators or for the supply of the neutron tubes described in the previous article are produced with the aid of either a Van de Graaff generator or a Greinacher cascade generator. In the latter, the voltage delivered by a high-tension transformer is rectified and multiplied by means of a suitable arrangement of rectifiers and capacitors in series and in parallel with one another [1]) (*fig. 1a*). The cascade generator can deliver considerably higher currents than the Van de Graaff generator, and moreover has the advantage of containing no moving parts which are subject to mechanical wear.

The conventional construction of cascade generators follows directly from the circuit of fig. 1*a*, and consists of two columns containing high-tension capacitors, interconnected as shown by rectifiers (tubes or semiconductor diodes). The spacing between the two columns and between successive stages of the cascade must be sufficient to preclude flashover and to keep brush-discharge losses within reasonable limits. As a consequence, the dimensions of a cascade generator for e.g. 150 kV are so large that as a rule a separate room is needed for it. In order to increase the attainable voltage or to reduce the dimensions, modern high-tension generators are frequently built in a pressurized vessel filled with a gas which diminishes the brush-discharge losses [2]).

A very compact cascade generator can be built if use is made of modern insulating materials and of the technique of "potting" or encapsulation in resin. The construction of the experimental cascade generator for 100 kV and 200 μA shown above becomes clear when the Greinacher circuit of fig. 1*a* is redrawn as in fig. 1*b*. The generator components are then distributed over *three* columns [2]). Space is saved

---

*) Philips Research Laboratories, Eindhoven.

**) Formerly of Philips Research Laboratories, Eindhoven.

[1]) See also A. Kuntke, Philips tech. Rev. **2**, 161-164, 1937; T. Douma and H. P. J. Brekoo, ibid. **11**, 123-128, 1949/50 and A. C. van Dorsten, ibid. **17**, 109-111, 1955/56.

[2]) See also the third of the articles cited under [1]).

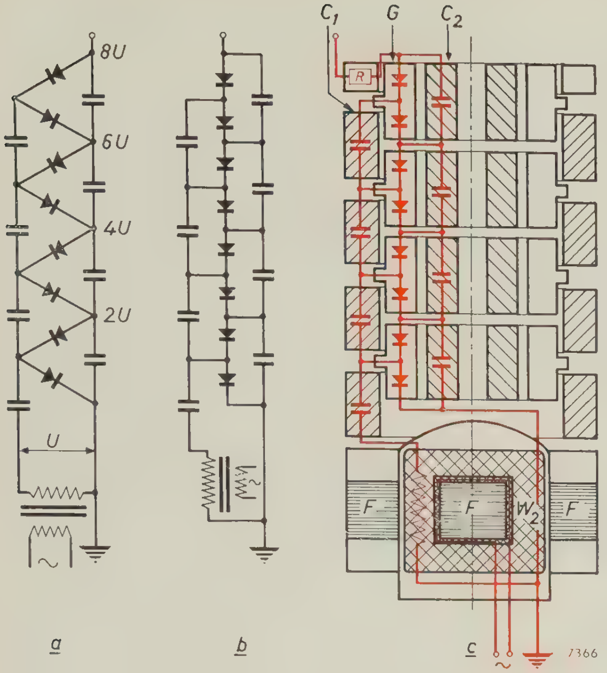

Fig. 1. *a*) Greinacher circuit for a cascade generator. The alternating voltage (of peak value U) is rectified and multiplied by a suitable combination of capacitors and rectifiers (tubes or semiconductor diodes); in the case shown here, the DC output voltage has a value of $8U$.
b) The Greinacher circuit drawn in a somewhat different way: the components are now distributed over *three* columns.
c) Sketch showing the construction of the miniature cascade generator shown in the title picture. Two tubular columns containing capacitors (C_1 and C_2) and one containing rectifiers (G) are fitted coaxially into one another. W_2 high-tension winding of the transformer. F iron core. R damping resistor. In order to make it easier to recognize the individual components, the Greinacher circuit as drawn in fig. 1*b* is also shown here, in red. The insulation is provided by insulating foil and by encapsulation in cast resin; the whole generator is moreover built into a tube filled with transformer oil.

by building these three columns as hollow cylinders and fitting them coaxially, as shown in the sketch of fig. 1*c* and the photo of *fig. 2*.

The capacitors consist of rolled-up sheets of aluminium foil and high-tension insulation foil, and are impregnated with transformer oil during the winding process. The rectifier unit (shown more clearly in *fig. 3*) consists of 2×175 silicon diodes of type OA 202 in a helical series arrangement, embedded in resin. The high-tension transformer is adapted to the cylindrical form of the other components, its laminations being circular. The windings of this transformer are also encapsulated in resin. The entire four-stage generator is finally placed in a PVC tube filled with transformer oil. The annular space left above the outer capacitor of the last stage of the cascade contains a damping resistor of about 100 kΩ (R in fig. 1*c*). This resistor is built up of a helical arrangement of smaller resistors encapsulated in cast resin, like the rectifier unit shown in fig. 3. The entire cascade generator without its earthed metal sheath is 80 cm long and has a diameter of 9.6 cm. It is designed for operation on a mains frequency of 50 c/s. The same principle can of course be used for generators for higher frequencies; the dimensions can then be even smaller, because of the smaller capacitances needed.

Most casting resins on the market have excellent insulating properties, but poor thermal conductivity. The permissible loading of high-tension generators insulated with casting resin is limited by this factor.

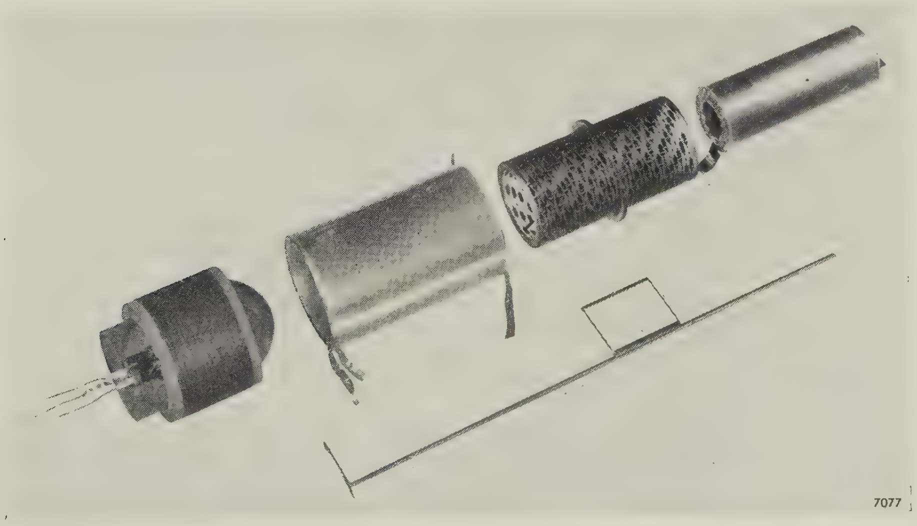

Fig. 2. The first stage of the high-tension cascade generator before assembly. The transformer, which is encapsulated in resin, is designed for 12.5 kV and 50 c/s; the output voltage of the first stage is then 25 kV DC.

A continuous load of 20 W, i.e. 200 μA at 100 kV, is however permissible in the present case.

The generators we have built deliver a high tension of positive polarity. A negative polarity can however easily be obtained by placing the transformer and the first of the outer capacitors at the other end of the column. (The damping resistor must then also be shifted.)

The title picture shows the generator in use, connected to a load resistor.

Miniature high-tension generators of this type may be used for many purposes in research and industry. A particularly important application is in combination with the neutron tube described in the previous article for oil-well logging (testing for the presence of oil-bearing strata in deep borings). The diameter of the high-tension generator must then be matched to that of the neutron tube so that they can both be lowered into the bore-hole. The use of long high-tension cables would then be obviated. We have so far reached an external diameter of 10 cm (*fig. 4*); the object is to reduce the diameter to 7 cm, i.e. that of the neutron tube in its definitive form.

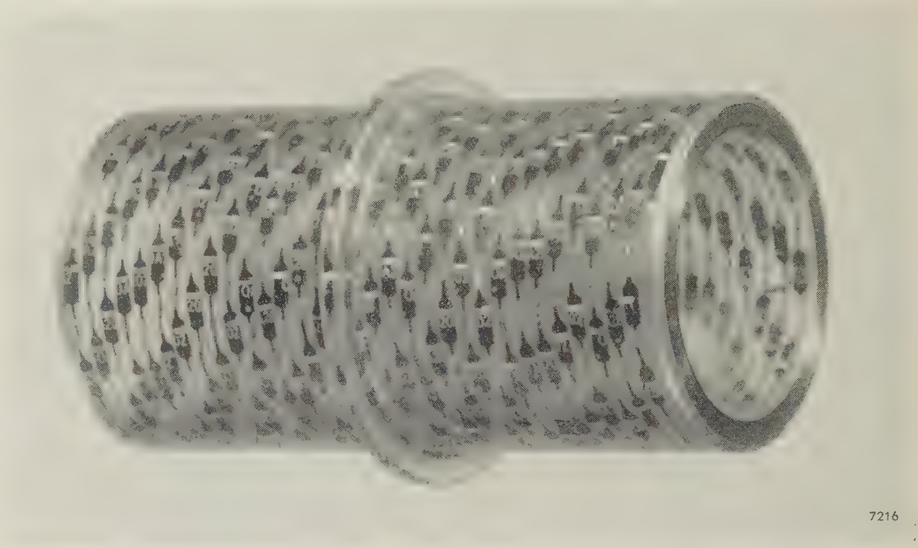

Fig. 3. A rectifier unit of the cascade generator. 2×175 silicon diodes type OA 202 are arranged along a helix and are encapsulated in resin for high-tension insulation.

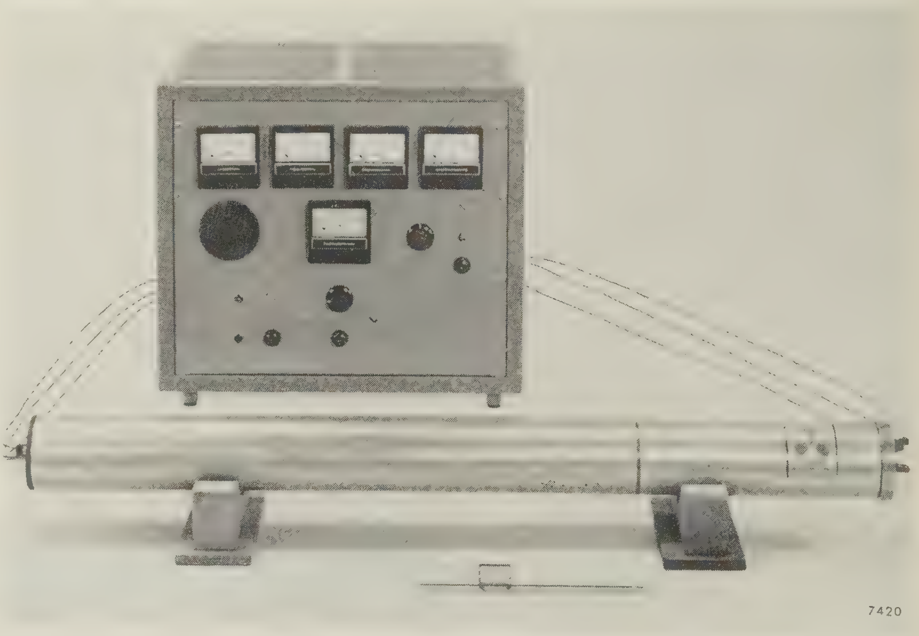

Fig. 4. Combination of the experimental high-tension generator and the neutron tube described in the previous article by Reifenschweiler and Nienhuis; both are built into an insulating tube with an earthed sheath (diameter 10 cm), the cascade generator on the left and the neutron tube on the right. The line drawn on the tube shows the position of the target; the radiation-hazard sign refers only to the tritium in the neutron tube. The ancillary current supply and control equipment may be seen in the background.

Such a combination would be very useful when the neutron tube is used for oil-well logging, since it would obviate the use of a high-tension cable.

Summary. Description of a four-stage Greinacher cascade generator, for 100 kV and 200 μA, built in the shape of a cylinder. It has a diameter of 9.6 cm (with earthed sheath, 10 cm), and a length of 80 cm. The compact construction is made possible by dividing the generator into *three* columns, which are given a tubular form and fitted coaxially. The insulation is provided partly by insulating foil, partly by encapsulation in resin. The generator is designed for use with a mains frequency of 50 c/s; for higher frequencies, an even smaller generator can be constructed on the same principle. Attempts are being made to reduce the diameter still further, to that of the Philips neutron tube (7 cm), so that the two together can be lowered into bore-holes for the purposes of oil-well logging.

ADJUSTING THE ION BEAM IN A PARTICLE ACCELERATOR

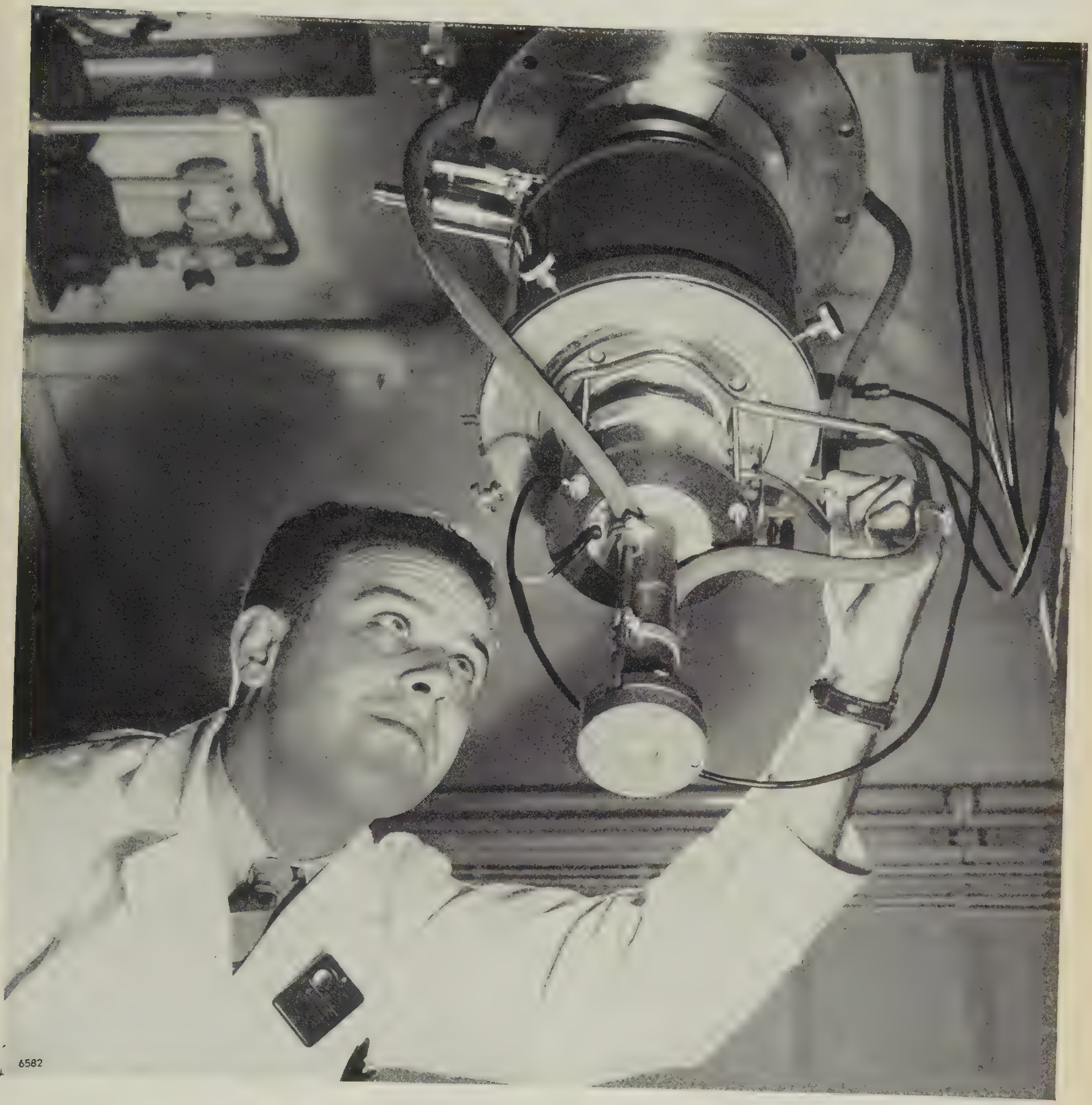

Photo Maurice Broomfield

In nuclear research "large" accelerators are used, such as cyclotrons and synchrocyclotrons, and also various "small" types, capable of accelerating particles up to an energy of 1 MeV. In these small accelerators the target section, which should be readily accessible, is usually located in a room below that containing the high-tension generator. The photograph shows the target section of an accelerator of this kind (cascade generator in a pressure tank), made by Philips for an institute of nuclear physics. If the ions are accelerated with a relatively low voltage, it is permissible to remain near the target, and the luminous beam of ions can then be seen through a glass insulator. By introducing into the beam a quartz plate attached to a spindle, as is being done here, the area struck by the beam is brilliantly illuminated. The target can then be accurately positioned with respect to the ion beam by means of four adjusting screws (three of which are visible on the photograph). A vacuum lock above the adjustable target section makes it possible to admit air into this section and to change the target whilst maintaining the vacuum in the accelerator itself.

The simple water-cooled target shown here, which serves for measuring the target current, can be replaced by, for example, a rotating target of heavy ice, cooled with liquid air. When bombarded with deuterons of 800 keV this target is able to deliver up to 10^{10} neutrons per second ¹), produced by the reaction D(d,n)^{3}He.

---

¹) A. C. van Dorsten and J. H. Spaa, A high-output D-D neutron generator for biological research, Nucl. Instr. **1**, 259-267, 1957.

MANUFACTURE AND TESTING OF ENAMELLED WIRE

by R. J. H. ALINK *), H. J. PEL *) and B. W. SPEEKMAN **).

621.315.337

Enamelled wire, which is used for winding coils, is at present one of the basic materials of the electrical industry. The present article gives a short survey of its manufacture, methods of testing and of the problems connected with the chemical and physical structure of the insulating lacquer.

One of the basic materials of the electrical industry is insulated copper wire, used for winding coils, transformers, rotors, stators etc. Originally copper wire surrounded by e.g. rubber or cotton was used for this purpose, but nowadays enamelled copper wire (more accurately "enamel lacquered wire") is used almost exclusively. The great advantage of insulating with enamel is that a very thin layer of the insulator is sufficient, so that coils with a relatively high "space factor" (i.e. coils in which a relatively large part of the volume is taken up by copper) can be obtained.

The variety of demands made on enamelled wire in the electrical industry has led to the development of a number of types differing in the chemical composition of the enamel layer. Pope's factory in Venlo (Netherlands) makes mainly the following four types:

a) Oil-laquer enamelled wire, the oldest type of enamelled wire [1]);
b) "Povin" wire, which is very strong;
c) "Posyn" wire, which can be easily soldered: the layer of enamel is readily removed when the wire is dipped into molten solder;
d) "Potermo" wire, which is resistant to quite high temperatures (up to about 155 °C).

All the above-mentioned types of wire are manufactured in more or less the same way, starting from chemically different lacquers. This article starts with a brief description of the manufacturing process. We shall then consider the demands which are made on enamelled wire, and the methods of testing whether these demands are met with. After this section, which deals with the practical side of the matter, follows a theoretical discussion of the relationship between the most important properties of the various types of wire and the structure of their insulating layer. Finally we shall pay special attention to a recent investigation which illustrates the presence and the danger of microscopic "flaws" in the enamel layer.

Manufacture

The manufacture of good enamelled wire entails applying the lacquer as *thinly* as possible to the wire, as otherwise it collects in drops and is thus unevenly distributed over the wire. It is therefore necessary to apply a number of coats of lacquer one after the other to get the required insulating thickness, which may be e.g. 16 μ for a copper wire 0.1 mm in diameter. The usual procedure is to pass the wire a number of times alternately through a lacquer reservoir and a muffle furnace: when it passes through the lacquer reservoir, the wire is covered with a thin coat of liquid lacquer; it is then dried ("muffled") in the furnace, returned to the reservoir for a new coat of lacquer, and so on, until the enamel layer has the desired thickness.

The machines which are used for this process may mainly be divided into two types: those in which the wire is led *vertically* through the furnace, and those in which it is led *horizontally*. Machines of these two types are shown in *figs 1* and *2* respectively.

Certain characteristic differences between the two types may be seen from these figures. The following will help to clarify these differences.

The force of gravity makes a horizontal wire lie in a slight curve (a "catenary"), which has undesirable consequences for the manufacture. The furnace of the horizontal machine must therefore be relatively short. Vertical machines, where this difficulty does not arise, can use furnaces 10 metres or more in length. The short horizontal machines have the advantage that the wire can be threaded through by one man, while the attractive point of the vertical machines is that, for

---

*) Philips Research Laboratory, Eindhoven. — Our late colleague Dr. Alink, who died in 1959, had as part of his work carried out a series of investigations on enamelled wire. The results of these investigations form part of the material of this article.

**) Pope's Wire and Lamp Factory, Venlo, Netherlands.

[1]) See e.g. J. Hoekstra, Philips tech. Rev. 3, 40, 1938.

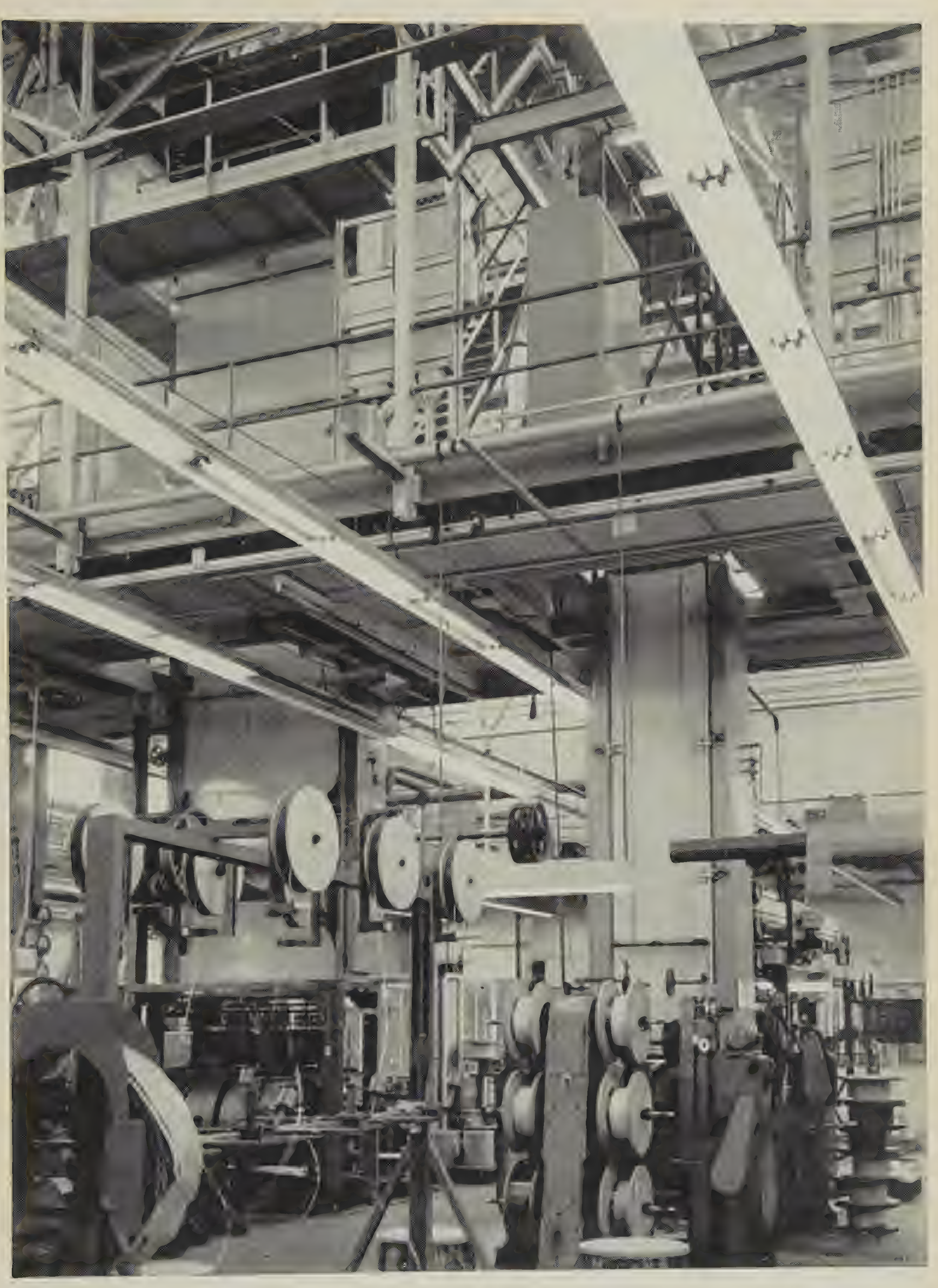

Fig. 1. Two *vertical* machines for the manufacture of enamelled wire. The one on the left is 14 m high. Each of these machines processes a number of wires at a time, each wire passing a number of times alternately through a lacquer reservoir and a muffle furnace. See also figs. 3 and 4.

a given drawing rate, the wire remains longer in the furnace. This is especially important with *thick* types of wire, where the lacquer is applied in relatively thick coats, and which therefore need rather a long drying time.

In general it is desirable for economic reasons to let one machine process a number of wires at a time. The advantage of this will however be lost if the wire breaks often, and if the whole machine has to be stopped each time a break occurs. Thick wire does not break very often, but with thin wire this possibility must indeed be kept in mind. As a logical conclusion, the manufacture of enamelled wire has tended towards the use of horizontal machines for thin wires, with one wire per machine (fig. 2), and multiple vertical machines for thick wire, taking 8 or more wires at a time (fig. 1).

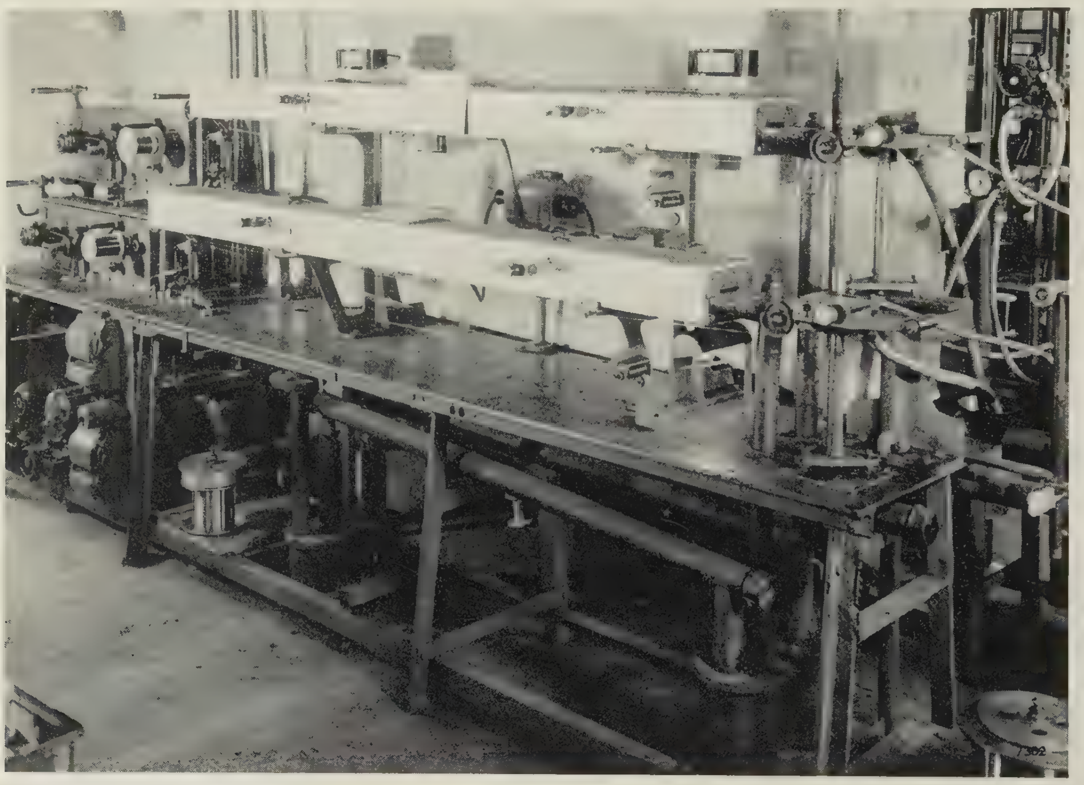

Fig. 2. Two *horizontal* machines for the manufacture of enamelled wire, placed one above the other. In each machine, the wire is passed a number of times alternately through a lacquer reservoir and an oven.

Figures 3 and *4* show some details of a vertical machine which enamels 16 wires at a time, applying 6 coats of lacquer to each wire. Fig. 3 shows the lacquer reservoir at the bottom of the machine. We see here $6 \times 16 = 96$ slits in the slanting wall through which the wires are drawn up via a roller to the furnace. It is inevitable that a small stream of lacquer will flow out through these slits; this ends up in a gutter, whence it is pumped back into the reservoir.

Fig. 4 shows the part of the machine where the 16 finished wires are "coiled".

Demands made on the wire and methods of testing

The finished wire is tested as regards a considerable number of properties. The *uniformity of the enamel layer* is of prime importance for wire to be used for winding purposes: the enamel must not show any inhomogeneities or pits, and must be applied equally thickly all round the copper. The mechanical, electrical and chemical properties of the enamel layer are also of great importance. We shall mention a few of the methods described in standard specifications for the testing of enamelled wire in these respects.

Holes and other large flaws in the insulation are detected by passing the wire through a conducting liquid (mercury or a solution of common salt), while a voltage is applied between the core of the wire and the liquid. The circuit also contains a resistor, a neon lamp and a counter. If the resistance of the enamel layer in contact with the liquid is less than e.g.

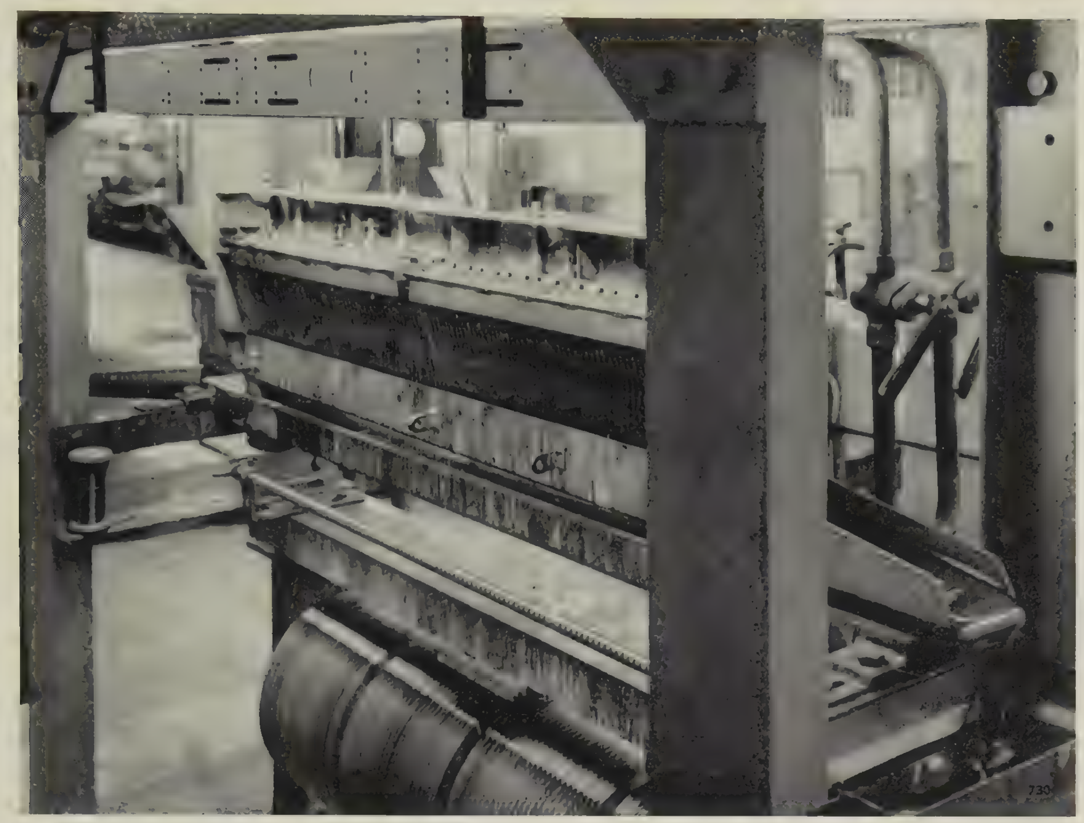

Fig. 3. The lacquer reservoir for a vertical machine. This machine supplies 16 wires at a time with a six-coat insulating layer. We see here how the wire is drawn up through 96 slits in the wall to the muffle furnace above. The thin stream of lacquer which flows out of these slits is caught in a gutter and pumped back to the lacquer reservoir. The degree of "muffling" is judged with the aid of a colour sample (the reel on the left): the colour of the enamelled wire is darker if the wire is muffled at a higher temperature or for a longer time. If the colour is lighter or darker than that of the sample, the rate at which the wire is drawn through the machine is decreased or increased, respectively.

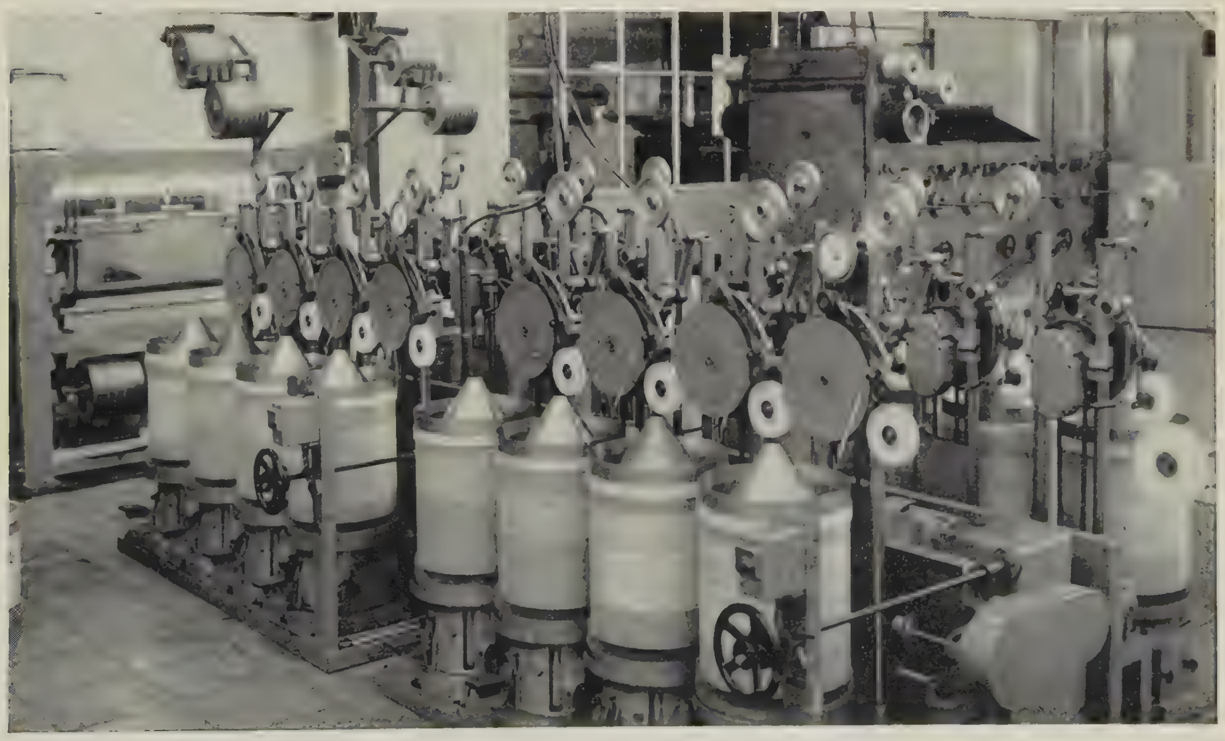

Fig. 4. Rotating containers in which the 16 finished wires coming from the machine in the background are "coiled".

10 000 Ω anywhere, a current flows through the circuit which lights up the neon lamp and sets the counter in operation (see *fig.* 5).

A uniform thickness of the enamel layer is of importance not only in connection with the insulation resistance, but also because a very constant wire diameter (standard deviation of less than 2%) is demanded for certain winding methods. We shall not discuss here the fairly simple methods used for testing the thickness of the wire.

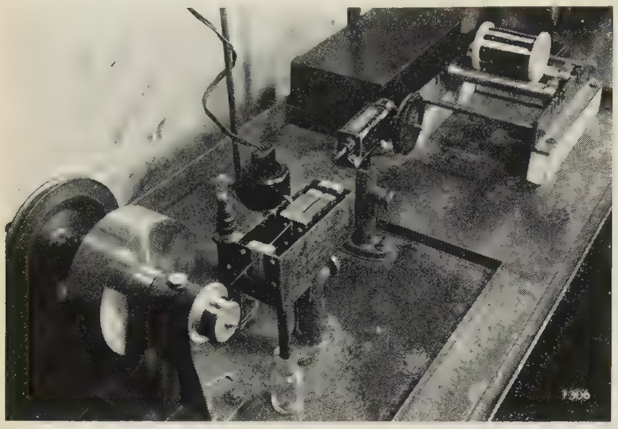

Fig. 5. An apparatus for detecting (fairly big) flaws in the insulation of enamelled wire. The motor on the left draws the wire under investigation through a tray containing mercury. The mercury and the core of the wire are connected in a circuit together with a neon lamp and a counter. Flaws in the wire passing through the mercury, i.e. places where the insulation resistance is less than 10 000 Ω, make the lamp light up and actuate the counter.

In order to check the layer structure of the enamel insulation simply and rapidly, the wire in question is placed for about 1 minute at an angle of 45° in a reagent which is capable of dissolving the enamel. A slanting cross-section of the enamel is then to be seen on the wire, and the various layers can be clearly seen with the aid of a magnifying glass (*fig.* 6).

The *mechanical* tests cover such diverse properties as resistance to wear, flexibility, etc. There are, for example, wear tests in which the number of strokes of a loaded reciprocating needle which the insulation can stand is determined. The flexibility and "windability" are tested by winding the wire round pins of roughly the same diameter as the wire itself. It is also stipulated that the wire after being wound in this way remains undamaged if the temperature is suddenly increased. This demand, which is one of the most stringent with which the wire must comply, is mainly of importance in connection with treatment which a coil may undergo after it is wound ("compounding" or impregnating).

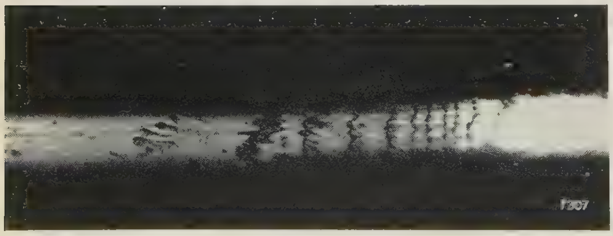

Fig. 6. A piece of enamelled wire in which the insulating layer has been etched off at an angle. The different coats in which the lacquer was applied can be clearly seen.

As far as the *electrical* properties of the enamel are concerned, the breakdown voltage in particular is of importance. This can be determined e.g. by winding a piece of wire round a polished steel cylinder, and applying a gradually increasing voltage between the core of the wire and the cylinder. Other electrical properties which it is desirable to know are the insulation resistance and the dielectric losses. Measurements of the insulation resistance carried out as an aid in the investigation of the physical structure of the enamel layer are discussed on p. 349.

The *chemical* properties of the enamel which are of special interest to the electrical engineer are the thermal aging and the resistance to solvents and impregnating agents. We shall mention thermal aging again briefly towards the end of the article, but for the rest we will leave this subject here: any further details would carry us too far into the practical aspect of the investigations. We shall now consider enamelled wire from a theoretical point of view.

Relationship between the chemical structure and the properties of the enamel layer

It is a difficult but rewarding task to try to find some relationship between the observable properties of enamelled wire and the chemical composition of the enamels used. We are far from having a complete insight into this matter, but what has already been reached is worthy of mention.

General principles of the structure of lacquer enamels

Lacquers may be divided into two groups: *physically drying* and *chemically drying*.

A physically drying lacquer consists of a volatile solvent with a macromolecular substance, e.g. nitrocellulose, dissolved in it. When such a lacquer is applied to an object, the solvent evaporates and the residue forms a layer on the object in question. This process takes place without any chemical change, i.e. the molecules do not react with one another. The enamel layer thus formed can be redissolved in the original solvent, and also has a tendency to soften when heated. These lacquers are therefore also sometimes called *thermoplastic* lacquers.

An enamel layer with entirely different properties is obtained if the molecules of the lacquer in question do react with each other, forming a three-dimensional network, as is the case with the chemically drying lacquers. The layer thus formed will not have the tendency to soften on heating, and is resistant to the usual solvents (though it may swell to a certain extent in some cases).

It will be clear that only the second type of lacquers, which are also known as *thermosetting* lacquers, come into consideration for use as insulation for wire. Thermoplastic lacquers are sometimes used as an *extra layer* on a wire which is already insulated with a thermosetting lacquer ("Thermoplac" wire). When a coil wound with this wire is heated, the outer layer will soften and thus cause the windings to stick together. This is useful e.g. in coils which must be given a rigid form without a support, such as the deflection coils in television picture tubes. In what follows, however, we shall forget about such thermoplastic lacquers, and only discuss the real insulating layer, which must thus comply with the above-mentioned condition that the molecules form a three-dimensional network.

A second necessary condition is that the network in question must adhere firmly to the copper. This can be explained as follows. It is of course essential that the enamel layer on wire used for winding coils should be able to accommodate the *strain* induced by the winding process without rupture. The copper core itself can meet this demand, as long as it is made in the right way. Now experiments have shown that a "loose" film of enamel can accomodate hardly any strain; instead, local constrictions are produced in the enamel, leading to breakage. If however the molecular network adheres rigidly to the copper everywhere, the enamel layer can easily be stretched with the copper without breaking.

We shall discuss a third general "structural principle" of lacquer enamels with reference to the oldest type of lacquer, oil lacquer.

Oil lacquers are made according to a principle going back to the last century for the preparation of e.g. carriage lacquer. The main ingredients of such lacquers were naturally occurring *resins* (rosin, copals) and *drying oils* (linseed oil, tung oil). Modern wire enamels with an oil base still use natural drying oils. The natural resins have however been replaced by synthetic resins, which gives the advantages of a more constant composition and a wider possible range of properties.

In the new oil lacquers as well as in the old ones we find an important structural principle, which is manifest to some degree in all types: there is a certain balance between the ingredients of a *flexible* nature and those of a more *rigid* nature. The first are here represented by the drying oils with their long linear carbon chain, the second by the resins, whose molecules contain a large number of rings (see *fig*. 7).

If the molecular network in question is formed only of the flexible components, as in e.g. rubber, we obtain a very elastic product, which however has the disadvantage of being soft and liable to swell in many solvents: molecules of the latter can easily penetrate the "open" network and cause it to expand. On the other hand, if the network is formed only of rigid components (as e.g. in certain synthetic resins) the result is a hard but brittle substance.

The combination of resins and drying oils actually used is just what is needed to give enamelled wire its excellent properties for use in winding coils: the enamel combines good flexibility with a considerable resistance to mechanical and chemical effects.

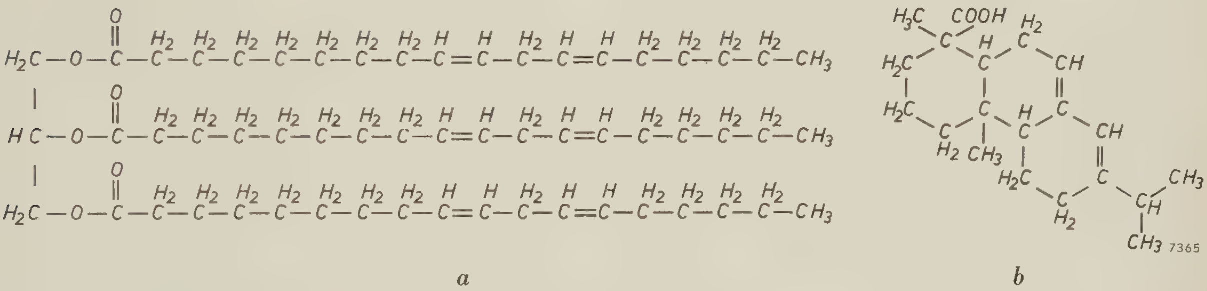

a *b*

Fig. 7. The chemical structure of *a*) an oil ingredient of oil lacquer (the glycerol ester of 9,12-linoleic acid) and *b*) of a resin ingredient (abietic acid).

Now that we have learnt some general structural principles, we may show how the individual properties of certain types of enamelled wire can be understood against their structural background.

"Povin" wire

As our first example we shall consider the entirely synthetic lacquer for "Povin" wire. This lacquer also has two main ingredients, which show the above-mentioned balance of properties. The first ingredient is polyvinyl formal, whose molecule is characterized by *a*) a mainly linear structure, *b*) the occurrence of ring systems of the 1,3-dioxane type, and *c*) a large number of hydroxyl and acetate groups (see *fig. 8*). The second ingredient is a synthetic resin marketed under the name "Novolak". Of this substance we need only mention that its molecule is mainly made up of rigid components and also contains a number of hydroxyl groups.

It is not yet quite clear what chemical reaction takes place between these two ingredients during the manufacturing process. It is assumed that the hydroxyl groups of the "Novolak" as well as those of the polyvinyl formal play a part in the formation of the three-dimensional network. This will not, however, contain a large number of chemical bonds, as in the case of oil lacquers: the chemical structure of the ingredients simply does not allow this.

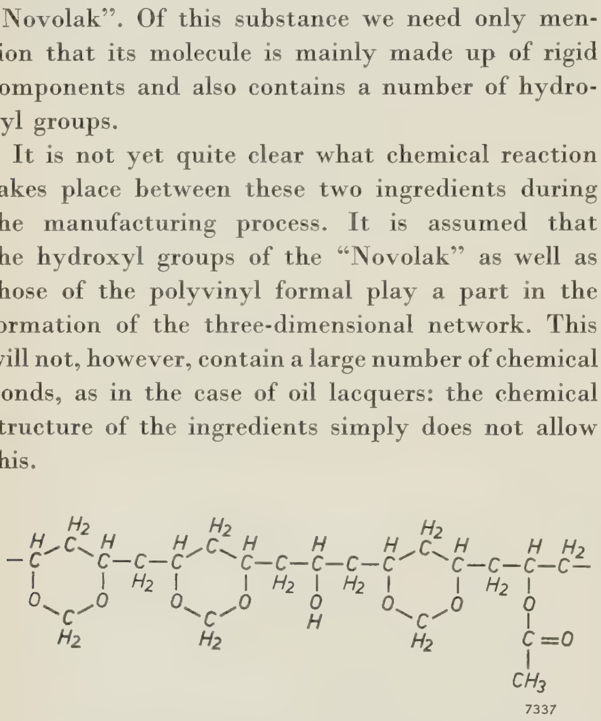

Fig. 8. The chemical structure of polyvinyl formal, an important ingredient of the insulation of "Povin" wire.

There is however plenty of opportunity for the formation of physical bonds, i.e. hydrogen bonds. These will be formed between the hydroxyl groups of the "Novolak" resin and the oxygen atoms in the dioxane rings of the polyvinyl formal.

Apart from the wide-meshed "loose" network of chemical bonds, a close-meshed network of hydrogen bonds will thus be formed. Each individual hydrogen bond is weaker than a chemical bond, but because of their great number a very strong structure results. Such a structure is just what is needed in a wire enamel: it may be expected that when the wire is bent, during which process the enamel layer is subjected to considerable strain, many of the quite weak hydrogen bonds will be broken. They will thus offer very little resistance to bending, while the breaking of the hydrogen bonds will lead to very little permanent damage: if the strain is relieved e.g. by heating for a short time, a new network of hydrogen bonds will immediately be formed, so that the old strength is regained. This is the reason for the excellent mechanical properties of "Povin" wire to which we alluded at the beginning of this article.

"Posyn" wire

As mentioned, the particular property of "Posyn" wire is that its enamel layer can be removed by dipping in molten solder. Here too, the connection between this property and the chemical structure of the enamel layer may be clearly seen.

The chemical bonds which hold much of the network together are formed by the reaction:

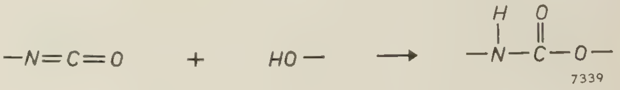

$$-N{=}C{=}O \quad + \quad HO- \quad \longrightarrow \quad -\overset{H}{\overset{|}{N}}-\overset{O}{\overset{\|}{C}}-O-$$

i.e. the reaction between an isocyanate group and a hydroxyl group. Now this reaction is a reversible reaction, which proceeds in the opposite direction at high temperatures. When the wire is dipped in the molten solder, the three-dimensional network breaks up into fragments of low molecular weight as a result of the reversal of this reaction. These fragments evaporate, and the copper which is thus exposed comes out of the solder bath covered with solder.

"Potermo" wire

The enamel of the recently developed "Potermo" wire has one of the least complicated network structures: the network is formed by the esterification of terephthalic acid with simple polyalcohols such as ethylene glycol and glycerol. The way in which the network is built up of these components is shown in *fig. 9*.

The excellent resistance to high temperatures of "Potermo" wire has been found by experiment to be due to the fact that oxygen from the air has very little effect on it. It is not entirely clear why a network like this should be so insensitive to oxygen, but on the other hand it is not altogether surprising: the network does after all consist practically entirely of benzene rings and ester groups, which are known not to react easily with oxygen. The other groups are probably sufficiently well shielded by the oxygen-resistant groups.

It is clear from the above what a complicated interplay of factors determines the quality of enamelled wire. In fact, the situation is even more complicated, because not only the structure itself, but also "flaws" in the structure have an influence on the quality. We shall devote the last section of this article to this important subject, in particular to an investigation in this field carried out in the Research Laboratories in Eindhoven.

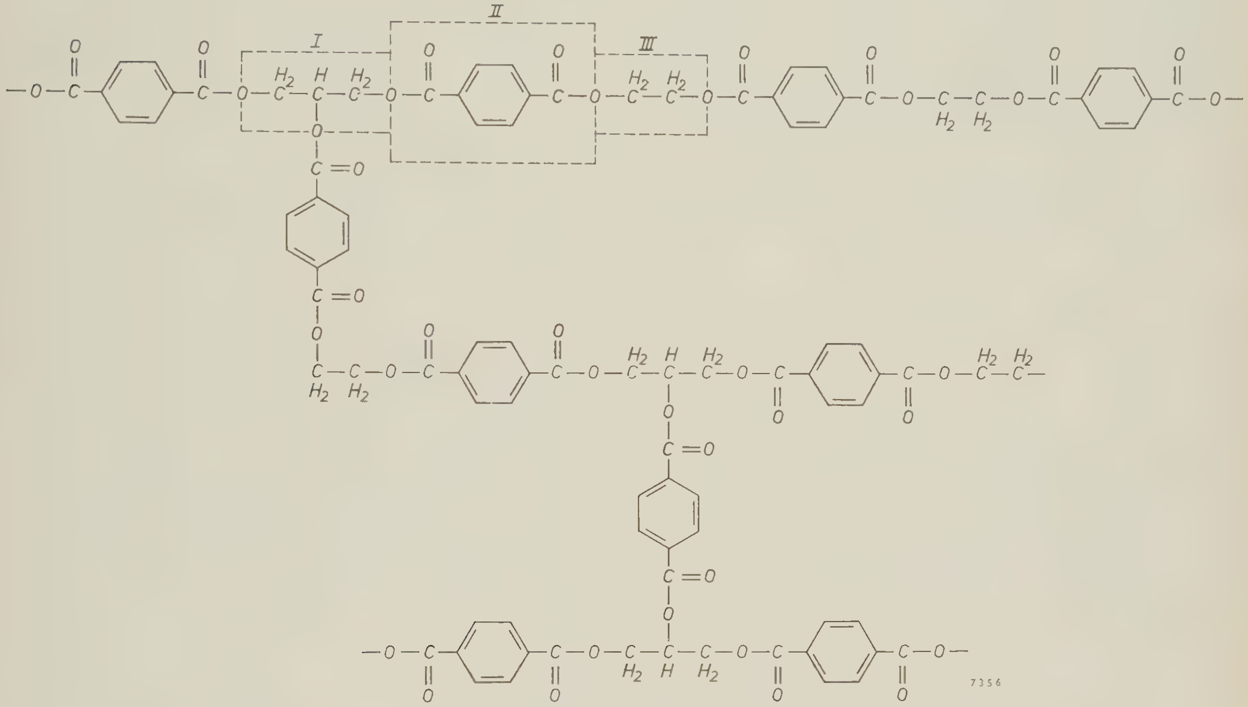

Fig. 9. The network structure of the insulation of "Potermo" wire. *I*: glycerol; *II*: terephthalic acid; *III*: ethylene glycol. These three components occur in various sequence in the network.

Investigation of "flaws" caused by mechanical stresses

It has been indicated in the foregoing how rather large flaws in the insulation are detected during the routine inspection of the wire. Work has been going on in the Research Laboratories over the past few years with a view to developing more refined methods for studying enamelled wire under mechanical stress. It has been found that measurement of the insulation resistance of the enamel layer, if carried out by sensitive methods, shows up the presence even of microscopically small cracks produced by such stress. Although this investigation has certainly not yet reached its final stage, the preliminary results fully justify great attention to this subject.

The first method used is based on measurement of the discharge time of a capacitor formed by clamping a metre of enamelled wire between tin foil. The tin foil is earthed, and the core of the wire connected to an electrometer. The capacitor so formed is charged to an known voltage, and the time needed for it to discharge to a certain lower voltage is measured. This time depends in a simple way on the unknown insulation resistance and on the capacitance, which is also unknown. In order to eliminate the latter unknown, a second measurement is carried out with a calibrated resistor included in the circuit in parallel with the capacitor.

Measurements on *dry* (and unstressed) enamelled wire gives a high value of the insulation resistance (e.g. 10^{13}-10^{14} Ω) for all types of wire, as long as there are no real holes in the enamel layer. Measurements on *damp* enamelled wire normally indicate a relatively small reduction in this resistance, the precise value of the reduction showing characteristic variations with the type of wire. The reduction increases in the order: oil-lacquer enamelled wire — "Posyn" wire — "Povin" wire.

This picture alters considerably as soon as the wire is subjected to bending tests, so that stresses are produced in the enamel layer. Even a slight bend (radius of curvature e.g. 1 m) in the wire produces a considerable reduction in the insulation resistance (e.g. by a factor 10-100) when the measurements are made on *damp* wire. If the wire is bent rapidly, or bent around a pin or a sharp corner, the effect is increased so much that the method is no longer applicable, because the capacitor discharges too fast.

The following method is used for further study of the problem. The core of the strongly bent wire is connected to the negative terminal of a battery, and the wire is dipped into a solution of common salt containing a little phenolphthalein. The other terminal of the battery is connected to a nickel rod which is placed in the same solution. Electrolytic effects are immediately produced: bubbles of hydrogen gas, together with OH^- ions, are produced at the bends in the immersed wire. The latter can be observed from the red colour assumed by the phenolphthalein at the *outer* side of each bend. This is what would be expected if one assumed that small cracks can be produced by tensile stress.

This method gives a negative result if the wire is only *slightly* bent, even after long periods of time, which surprised us at first.

Careful microscopic investigation finally produced a fairly complete picture of the nature of these flaws. When the wire is quickly bent round a pin, one observes cracks suddenly forming in the enamel layer after some time. Even if the wire is bent slowly and slightly, very fine cracks are observed after enough time has elapsed. These hair cracks, however, do *not* extend right through to the core, but are restricted to a few outer layers of the insulation. It may be assumed that such cracks do produce a considerable decrease in the resistance, but do not allow electrolytic effects to occur. If the enamelled wire is warmed, the hair cracks often close up again: they can then no longer be observed under the microscope, and the insulation resistance is observed to have increased again. The hair cracks can be regarded as fairly "harmless" precursors of the cracks produced by e.g. bending round a sharp angle.

Cracks of the latter type are most undesirable in a coil wound with enamel wire: if the coil is internally damp, they allow undesirable small currents to flow — i.e. they can cause a certain measure of short-circuiting. If such currents contain a DC component, they can also cause severe corrosion of the copper wire as a result of electrolysis. If the corrosion is allowed to proceed far enough, the copper wire may even break.

So much for this investigation. Its results throw an interesting light on various practical developments of recent times. For instance, for the winding of coils the *rectangular* cores and formers which were formerly common are being replaced more and more by ones with *rounded* corners. Moreover, attempts are being made to improve the quality of the coils by using *waterproof* materials for separating the windings.

As far as understanding of the above-mentioned phenomena is concerned, it will be clear that science still has a lot of ground to win from empirical knowledge in this field; and this is just what makes this subject so fascinating. There is thus no better way of closing this short survey of the work on enamelled wire than with the mention of a couple of examples which are still not easy to understand. *Fig. 10* illustrates the curious complications which are found in the thermal aging of enamelled wire. Quite un-

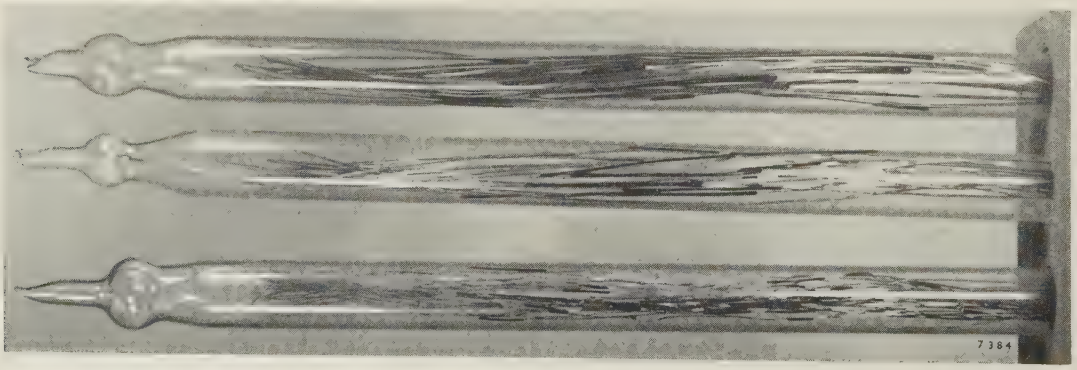

Fig. 10. Thermal aging of "Posyn" wire in a sealed tube for 48 hours at 180 °C. Surprisingly enough, the insulation is damaged more by thermal aging under these conditions than when it is exposed to the same temperature for the same time in air.

expectedly, "Posyn" wire in a sealed-off tube shows a more rapid deterioration of the insulation than the same wire which is simply exposed to the air. This phenomenon is found to a greater or lesser extent with all "solderable" wires. It is not so pronounced with "Posyn" wire, but it is still not entirely suppressed. *Fig. 11* shows a series of ring-shaped cracks which are produced when a bent piece of "Povin" or "Posyn" wire is dipped in a solvent. This phenomenon, which is called "solvent cracking", is very closely connected with the mechanical stresses present in the enamel layer: if the wire is heated to 100-120 °C after bending, so that the mechanical stresses in the enamel are relieved, solvent cracking does not occur. It is also very strange that such cracks are quite absent when oil-lacquer enamelled wire is used.

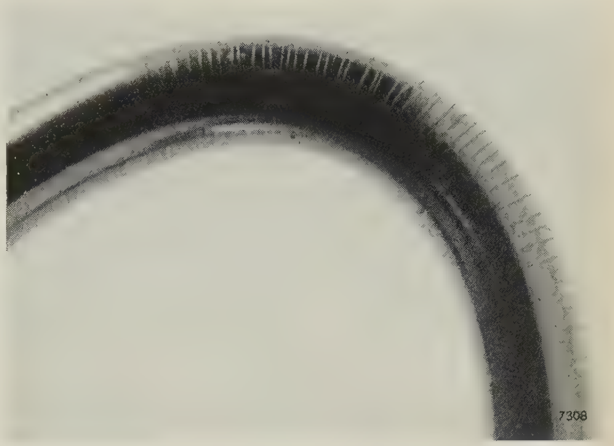

Fig. 11. A series of cracks (magnification 20×) in a piece of "Povin" wire, produced by bending the wire and dipping it into methanol. No really satisfactory explanation has yet been found for this "solvent cracking".

Summary. Among the properties required of enamelled wire used for the winding of coils are flexibility and resistance to mechanical and chemical effects. The "enamel" insulation consists of "chemically drying" lacquers, which are applied in several coats by passing the wire a number of times alternately through a lacquer reservoir and a muffle furnace. This process is carried out horizontally for thin wire but vertically for thick wire. To obtain satisfactory enamel layers the following conditions must be satisfied: *a*) the formation of a three-dimensional network of atoms which *b*) is firmly attached to the copper and which *c*) contains both flexible and rigid elements. The last requirement is illustrated for the case of oil-lacquer enamelled wire. Further, a theoretical explanation is given for the great mechanical strength of "Povin" wire, for the remarkable fact that "Posyn" wire can be soldered through the enamel layer, and for the thermal resistance of "Potermo" wire. Finally, a recent investigation of microscopic "flaws" produced by mechanical stress is described, and a number of phenomena which are as yet rather difficult to understand are mentioned.

THE PLOTTING OF ELECTRON TRAJECTORIES WITH THE AID OF A RESISTANCE NETWORK AND AN ANALOGUE COMPUTER

by A. J. F. de BEER *), H. GROENDIJK *) and J. L. VERSTER *).

537.533.3:621.517.729:681.14.001.57

Controlling the form of an electron beam is a problem frequently encountered in electronic engineering, for example in designing the focusing system of an electron microscope, an X-ray tube or a television picture tube. With the aid of a resistance network and an analogue computer the manner in which a very narrow electron beam is focused by an electrostatic lens can be ascertained quickly and accurately.

Determining the electron trajectories in the electric field of a given electrode configuration is a problem encountered in the design of many types of electron tube. The calculation of the fields and of the electron trajectories is very time-consuming work, and therefore various methods have been developed in the course of the years for speeding up the calculations involved. An elegant method of determining electron trajectories consists in rolling steel balls over a rubber membrane 1) 2). This method can only be used for "two-dimensional" fields and is therefore not suitable for most modern types of tubes. The electrolytic tank with automatic plotting mechanism, described some time ago in this journal 3), does not suffer from this limitation and is therefore generally useful for systems possessing rotational symmetry, such as the focusing lens of television picture tubes for example (*fig. 1*). It is less suitable, however, where the trajectories considered are close to the axis of such a system (paraxial trajectories), for the principle underlying the apparatus in question consists in calculating the curvature of the trajectory. The latter is always very small in the paraxial case, so that the relative error in the result is too great.

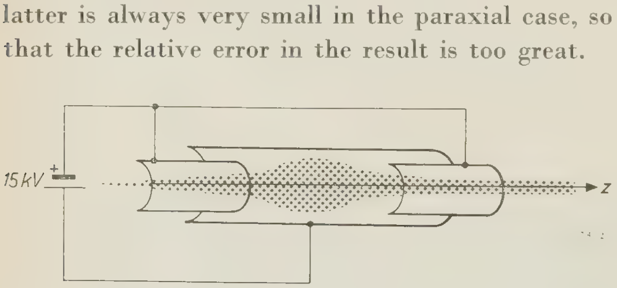

Fig. 1. Cross-section of an electrostatic focusing lens in a television picture tube. The lens consists of three coaxial cylinders at different potentials. The width of the electron beam is here exaggerated.

We shall now describe another method by which precisely the paraxial trajectories can be determined automatically and with sufficient accuracy. This method makes use of a differential equation which has the paraxial trajectories as solutions. The coefficients of the differential equation are functions of the potential Φ on the axis of the electrode system. The variation of Φ is found with the aid of a *resistance network* 4). A PACE *analogue computer* 5) produces the solutions of the differential equation. The solutions are traced by an x-y recorder. *Fig. 2* gives a view of the equipment employed.

Principle of calculating the trajectories

If z is the coordinate along the symmetry axis of the electrode system and r is the distance to this axis, then the differential equation for the trajectories $r(z)$ is:

$$4\,\Phi r'' + 2\,\Phi' r' + \Phi'' r = 0. \quad . \quad . \quad . \quad (1)$$

Here Φ is the potential at the axis, and the primes represent derivatives with respect to z. This equation, which contains as coefficients only the function Φ *on the axis* and derivatives of Φ *in the direction of the axis*, is derived from the general differential equation for the path of an electron for the special case of an electric field possessing rotational symmetry, and for r and r' both small (paraxial rays) 6). By substituting 7)

$$r = R\,\Phi^{-1/4} \quad . \quad . \quad . \quad . \quad . \quad . \quad (2)$$

---

*) Philips Research Laboratories, Eindhoven.

1) P. H. J. A. Kleynen, The motion of an electron in two-dimensional electrostatic fields, Philips tech. Rev. **2**, 338-345, 1937.

2) G. Alma, G. Diemer and H. Groendijk, A rubber membrane model for tracing electron paths in space charge fields, Philips tech. Rev. **14**, 336-344, 1952/1953.

3) J. L. Verster, An apparatus for automatically plotting electron trajectories, Philips tech. Rev. **22**, 245-259, 1960/61.

4) J. C. Francken, The resistance network, a simple and accurate aid to the solution of potential problems, Philips tech. Rev. **21**, 10-23, 1959/60.

5) This computer, made by Electronic Associates, Long Branche, N.J., has been installed in Philips Computing Centre at Eindhoven. W. P. J. Fontein and L. G. J. ter Haar of the Computing Centre helped to design the circuits for solving our problem and assisted in the experiments.

6) V. E. Cosslet, Introduction to electron optics, Clarendon Press, Oxford 1950, p. 36.

7) The letter R will also be used in this article to denote electrical resistance. As there was little risk of confusion, there was no reason to depart from this internationally accepted symbol in electron optics.

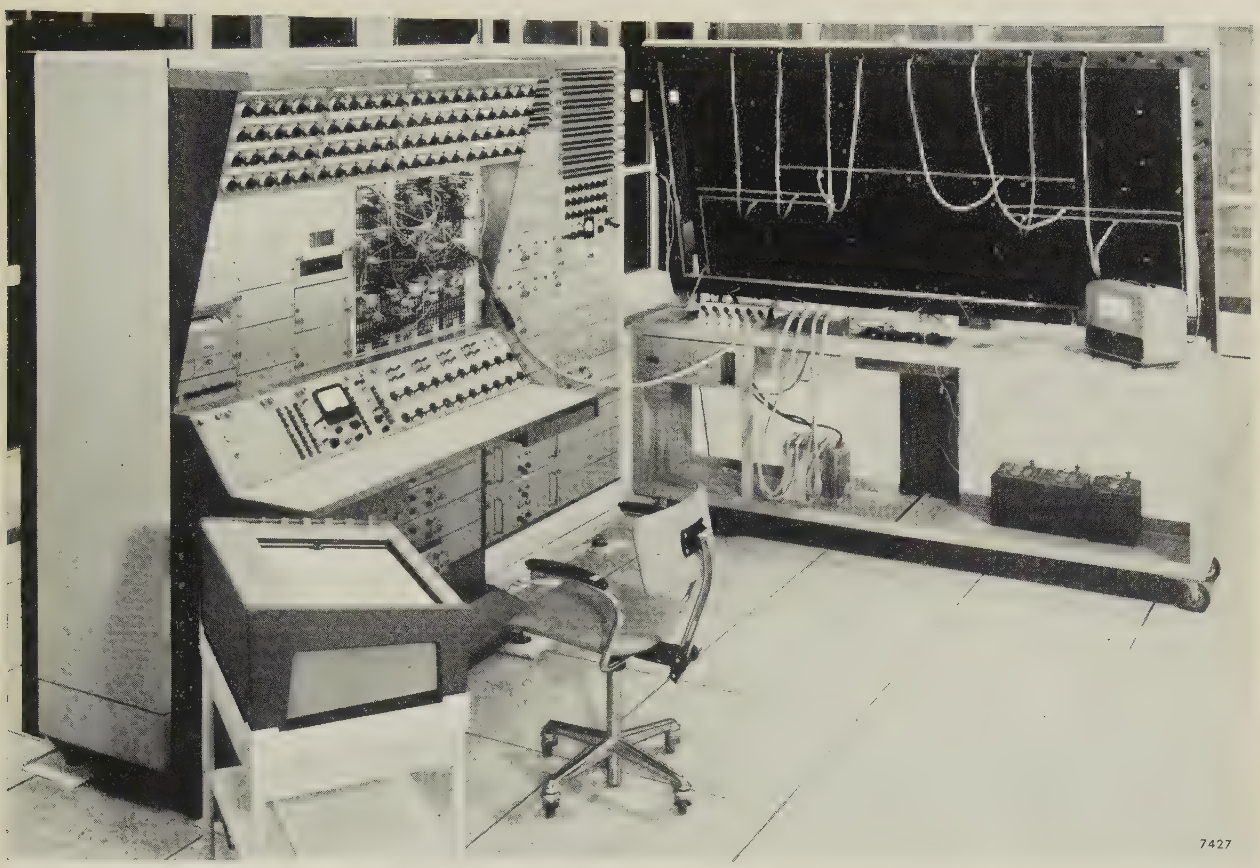

Fig. 2. View of the equipment for the automatic tracing of paraxial electron trajectories. On the right is the resistance network, on which the model of the investigated electrode system is marked, for clarity, with white cord. The cord is wound around the contacts of the network points, so that the mesh spacing is visible. The contacts themselves are too small to be seen on the photograph. On the left is the PACE analogue computer. The trajectories calculated by the computer are traced on the *x*-*y* recorder in the foreground.

the equation can be further simplified to Picht's equation:

$$R'' + \frac{3}{16}\left(\frac{\Phi'}{\Phi}\right)^2 R = 0. \quad . \quad . \quad . \quad . \quad (3)$$

This equation no longer contains the second derivative of Φ. Since, as a rule, second derivatives cannot be determined so accurately as first derivatives, the latter equation is to be preferred.

In order first to describe broadly the process by which the analogue computer solves this differential equation, we assume for the moment that $(\Phi'/\Phi)^2$ has a constant value K. The reader may accept provisionally that the machine can generate a voltage V which, as a function of time t, satisfies the equation analogous to eq. (3):

$$\frac{\mathrm{d}^2 V}{\mathrm{d}t^2} + \frac{3}{16} KV = 0. \quad . \quad . \quad . \quad . \quad . \quad (4)$$

This voltage is traced on an *x*-*y* recorder, the stylus moving at a constant velocity in the t direction. If we replace the V and the t axis of the graph thus produced by an R and a z axis respectively, we have one of the solutions of Picht's equation (3), i.e. that with the initial values R and R' corresponding to the preset initial values of V and $\mathrm{d}V/\mathrm{d}t$.

Since this is important to the understanding of what follows, it should be emphasized that in the machine the varying of the z coordinate is substituted by the passage of time, appearing in the fact that the stylus of the recorder moves at a constant speed in the z direction.

Now, in the case considered here the coefficient $(\Phi'/\Phi)^2$ is not constant but is a function of z. In order to construct the solutions in the same way with the analogue computer, the variation of $(\Phi'/\Phi)^2$ must be supplied to the machine in such a way that, at the moment during the solving process when an arbitrary point z_1 is reached on the z axis, the machine is supplied with a voltage whose magnitude is proportional to the value of $(\Phi'/\Phi)^2$ at z_1.

As mentioned, $\Phi(z)$ — from which $(\Phi'/\Phi)^2$ is calculated — is determined with the aid of a resistance network. For our present purposes we shall disregard in the first instance the fact that the resistance network only gives the potential at a number of discrete points along the axis; we assume, then, that the potential Φ can be *continuously* scanned by means of a sliding contact (*fig. 3*). The derivative Φ' along the axis can be approximated by

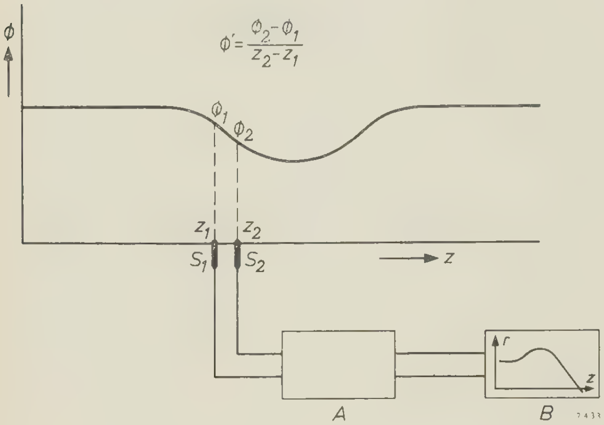

Fig. 3. Diagram illustrating the principle of the trajectory calculation. The potential along the z axis and its derivative are scanned with two sliding contacts S_1 and S_2. From the result the computer A calculates the variable coefficient $(\Phi'/\Phi)^2$ which occurs in Picht's equation, and solves that equation. B is the x-y recorder.

the quotient $(\Delta\Phi/\Delta z)$ of the difference between the potentials at two closely adjacent points, z_1 and z_2, and the distance between these two points. For this purpose we must use *two* sliding contacts, S_1 and S_2, moving along the same axis. A circuit in the computer itself divides by Φ the value of Φ' thus obtained, and squares the result. At the same moment at which the two contacts sliding along the z axis pass the points z_1 and z_2, the value of $(\Phi'/\Phi)^2$ pertaining to z_1 appears at the output of the circuit mentioned. (The "calculation" in an analogue computer takes no computing time.)

To ensure the above-mentioned time relation between $(\Phi'/\Phi)^2$ and $r(z)$, the contacts must move along the z axis at the same speed as the z coordinate is swept when finding the solution. A different speed means that, when the quotient $(\Delta\Phi/\Delta z)$ is computed, Φ is not differentiated with respect to z but with respect to, for example, az. This amounts to substituting $3/(16a)^2$ for the factor 3/16 in eq. (3), so that the wrong differential equation would be solved. In the following we shall consider how the required time relation is obtained. We shall also explain how, using the resistance network (with which, as mentioned, the function Φ cannot be continuously scanned) an approximate value of Φ and Φ' is determined by interpolation. An incidental problem, which will also be dealt with, concerns the method of ensuring that the coupling of the computer to the resistance network does not distort the correct potential distribution over the network.

The solution of these problems was well worth while. Hitherto it was necessary to measure the relevant voltages separately on the network and to compute each trajectory numerically; with some training, this took about two hours. The computer takes only a minute to do the same work.

Before dealing with the above questions, we shall discuss the principal elements from which the circuits in an analogue computer are built up.

Basic elements of an analogue computer

The adder

Fig. 4a shows the symbol used for an "adder" in analogue computer technique, and fig. 4*b* gives the circuit diagram. The triangle with curved base A represents an "operational amplifier", whose main features are a high gain (approx. 10^8) and the fact that it reverses the polarity of the voltage. Because of this there is virtually no voltage across the input i of the amplifier (potential of p equal to zero). If the input voltage were to differ slightly from this value, the result at the output u would be a very high potential of opposite polarity which, via the feedback resistor R_u, would again immediately reduce the input voltage to zero. Since the potential of p remains constant at zero, the currents V_1/R_1 and V_2/R_2, which arise when the voltages V_1 and V_2 are applied to resistors R_1 and R_2, cannot flow to earth. If they were to do so, they would produce across the input resistance of A a voltage that would make the potential of p differ from zero. The currents mentioned must therefore pass through the negative feedback resistance R_u. Let the output voltage be V_u, then:

$$\frac{V_u}{R_u} = -\left(\frac{V_1}{R_1} + \frac{V_2}{R_2}\right),$$

or

$$V_u = -\left(\frac{R_u}{R_1}\,V_1 + \frac{R_u}{R_2}\,V_2\right).$$

The result, then, is that the circuit multiplies V_1 and V_2 by the negative constants $-R_u/R_1$ and $-R_u/R_2$, respectively, and adds the products. Since the amplifier is used for this and other elementary mathematical operations, it has been given the name "operational amplifier".

If only one voltage V_1 is applied to the input, and moreover $R_1 = R_u$, what appears at the output is simply the same voltage of opposite polarity, $-V_1$. (The symbol in fig. 4*a* is then, of course, drawn with

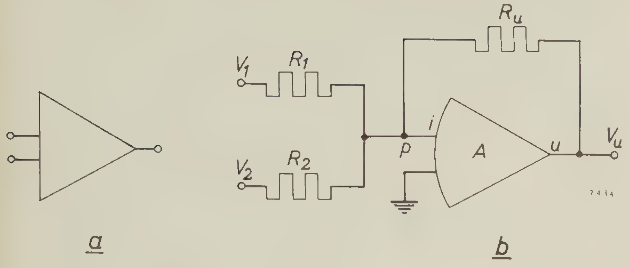

Fig. 4. *a*) Symbol and *b*) circuit diagram of adder in an analogue computer. As a result of the high negative feedback of the operational amplifier *A*, the point *p* remains at zero potential. Currents V_1/R_1 and V_2/R_2 have to flow together through the feedback resistor R_u because no perceptible current flows through the input resistance of *A*. When $R_u = R_1 = R_2$, then $V_u = -(V_1+V_2)$.

only one input.) If V_1 and V_2 are to be subtracted from one another, two operational amplifiers are needed: one to produce $-V_1$, and the other for the addition of the V_2.

The integrator

Fig. 5a represents the symbol of an integrator, and fig. 5*b* the relevant circuit diagram. The current V_1/R_1 must again flow entirely through the feedback circuit, which in this case contains the capacitor *C*. For the output voltage V_u we now have:

$$\frac{V_1}{R_1} = -C\frac{\mathrm{d}V_u}{\mathrm{d}t}$$

or

$$V_u = -\frac{1}{R_1 C}\int_0 V_1\,\mathrm{d}t + V_u(0).$$

In the latter expression $V_u(0)$ is the output voltage at the moment $t = 0$. By giving this voltage a specific value we can introduce the initial conditions of a differential equation. Choosing $R_1C = 1$ second, we find for V_u precisely the value of the integral of $-V_1$. By taking another value for *RC* we can multiply the value of the integral by a specific constant.

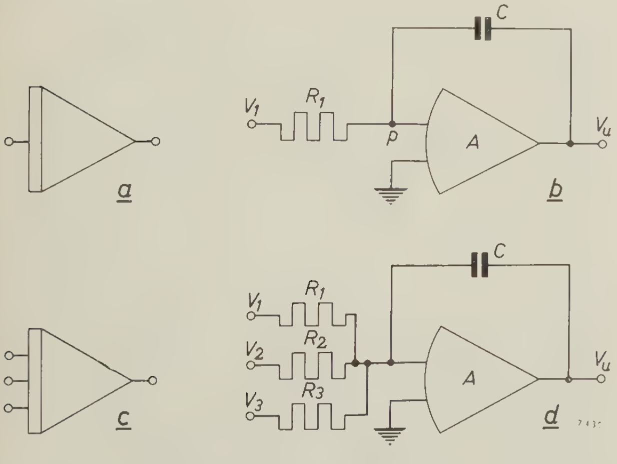

Fig. 5. *a*) Symbol and *b*) circuit diagram of an integrator. Point *p* again has zero potential. As in the case of the adding circuit, the current V_1/R_1 flows through the feedback circuit, which here contains the capacitor *C*. When $R_1C = 1$, then $V_u = -\int V_1 \mathrm{d}t$. *c*) Symbol and *d*) circuit diagram of an integrator which simultaneously adds and integrates: $V_u = -\int(V_1 + V_2 + V_3)\,\mathrm{d}t$.

In practice an integrator always has various resistors R_1, R_2, R_3, . . . at the input. If we apply to three of these resistors, for example, the voltages V_1, V_2, V_3 (fig. 5*d*, with the appertaining symbol in fig. 5*c*) and if we choose $R_1C = R_2C = R_3C = 1$ sec, we obtain at the output:

$$V = -\int (V_1 + V_2 + V_3)\mathrm{d}t.$$

The multiplier

Of the various kinds of multipliers used in analogue computers, we shall treat here only the kind known as *servo-multipliers*. The symbol and the diagram can be seen in *fig. 6*. Along the potentiometer P_1 the potential rises from zero to the "reference voltage" V_r, usually chosen as 100 V. The operational amplifier A_1 supplies an energizing voltage to the servo-motor *M* until the voltages at the two inputs i' and i'' are equal to one another, that is until the sliding contact of P_1 is at the point where the voltage is equal to V_1. The voltage-division ratio a on the potentiometer P_1 is then equal to V_1/V_r. Since the sliding contact of potentiometer P_2 is mechanically coupled to that of P_1, the voltage-division ratio on that potentiometer is now also equal to V_1/V_r. When a voltage V_2 is applied to P_2, the voltage on its sliding contact is $V_u = aV_2 = (V_1 \times V_2)/V_r$, that is to say, except for a constant factor, the product of V_1 and V_2.

To prevent this constant factor always appearing in the formulae, the actual computing voltage V [8]) is not used when designing the circuits but the quotient V/V_r. In this way, all computing voltages are normalized with respect to the reference voltage. In the following this normalization will be tacitly applied, and this should be borne in mind when considering the various formulae, since the normalization transforms the computing voltages into dimensionless quantities.

A multiplier usually contains several potentiometers, e.g. five, all sliding contacts of which are mechanically coupled to that of the first. It is then possible simultaneously to produce the products V_1V_2, V_1V_3, V_1V_4, and so on. If, for instance, we take for V_3 the product V_1V_2 already formed, we then obtain $V_1^2V_2$.

---

[8]) The term "computing voltage" is used to distinguish it from other voltages in the computer that have nothing to do with the computation.

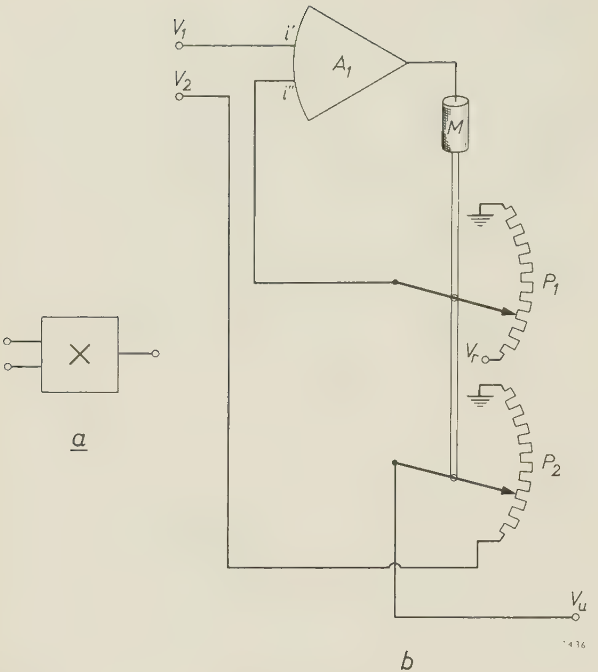

Fig. 6. *a*) Symbol and *b*) circuit diagram of a multiplier. M is a servo-motor which simultaneously drives the sliding contacts of potentiometers P_1 and P_2. The amplifier A_1 energizes the servo-motor until the voltages at both inputs i' and i'' are identical, that is until the sliding contact P_1 is at the point where the voltage is equal to V_1. The voltage-division ratio of both potentiometers is then equal to V_1/V_r, where V_r is a reference voltage. When a voltage V_2 is applied to the second potentiometer, the voltage on its sliding contact is $V_u = V_1V_2/V_r$, that is, except for a constant factor, the product of V_1 and V_2.

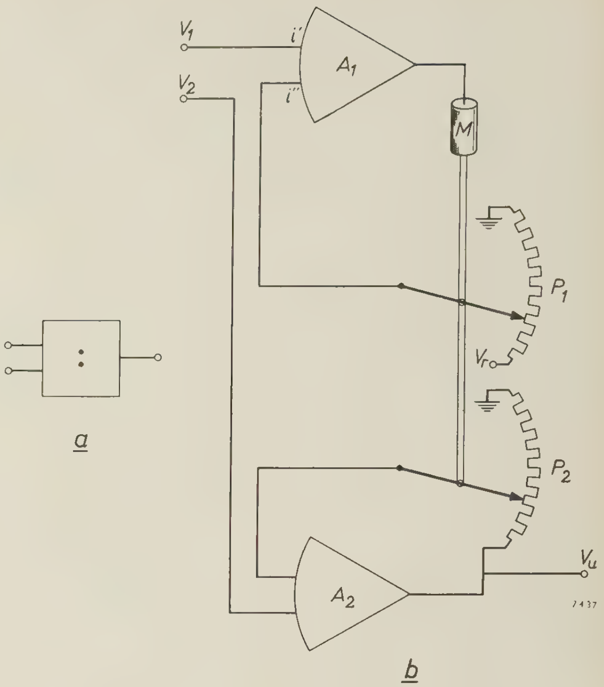

Fig. 7. *a*) Symbol and *b*) circuit diagram of a divider, which produces the quotient V_2/V_1. The position of the two sliding contacts is regulated in the same way as for the multiplier. The normalization applied makes the voltage division ratio on potentiometers P_1 and P_2 both equal to V_1. The operational amplifier A_2 ensures that V_u acquires a value at which zero difference exists between the voltages at its inputs. In that case $V_2 = V_1V_u$, and thus: $V_u = V_2/V_1$.

The divider

By means of the circuit in *fig. 7* the quotient V_2/V_1 can be obtained. The operation of the circuit is explained in the caption to the figure.

All the above-mentioned basic elements are electronic. It is also possible to use other basic elements, for example mechanical elements, as done for the first time by Bush in a computer for solving differential equations [9]). Mechanical analogue computers are often accurate enough, but they are relatively slow in operation.

Solving Picht's equation

To solve Picht's equation with the analogue computer, the equation is written in the form:

$$R'' = -\frac{3}{16}\left(\frac{\Phi'}{\Phi}\right)^2 R.$$

Two integrators I_1 and I_2 (*fig. 8*) are now connected in series, and R'' (in the form of a voltage varying with time) is applied to I_1. Between I_1 and I_2 one then finds $-R'$, and I_2 delivers the function R itself, which represents the solution. For the purpose of applying R'' to the integrator I_1, it is computed with the aid of the basic elements described from R and $(\Phi'/\Phi)^2$ in accordance with the equation in the above form.

It may be asked how this is possible, for R has only just been produced by integration from R''. We are not concerned here, however, with the performance of successive mathematical operations, but with a feedback circuit (a "loop") in which the currents flowing, governed by the basic elements, are such that the variation of the voltage V at the output gives a solution of the differential equation.

Since the circuit in fig. 8 satisfies the same differential equation (in the "computer variables" V and t) as applies to the electron trajectories $R(z)$ (with the "problem variables" R and z), it can be said that the circuit is an analogue for the behaviour of the electrons in the electric field. The name analogue computer expresses this kind of relationship. We have attempted above to prepare the reader for the perhaps somewhat confusing interplay between the computer variables V and t and the problem variables R and z (we shall henceforth largely be concerned with the latter).

---

[9]) V. Bush and H. L. Hazen, Integraph solutions of differential equations, J. Franklin Inst. **204**, 575-615, 1927. See also A. S. Jackson, Analog computation, McGraw-Hill, New York 1960. The latter book is recommended for a further study of the theory and application of analogue computers.

The computer contains a separate circuit with which the transformed trajectory coordinate R is retransformed in accordance with (2) into the actual trajectory coordinate r, thus immediately giving the solution in the required form.

When the capacitors in the integrators are charged to the voltages corresponding to the chosen initial values, the computer is set in operation by the simultaneous closing of a number of switches. The sliding contacts then immediately begin to sweep the z axis of the network, and the recording stylus begins to trace the solution. At every point z_1 the deflection of the stylus in the y direction is proportional to the value of the trajectory coordinate r in z_1. After roughly one minute, the contacts reach the end point; the recorder has then traced one of the solutions of the differential equation (1).

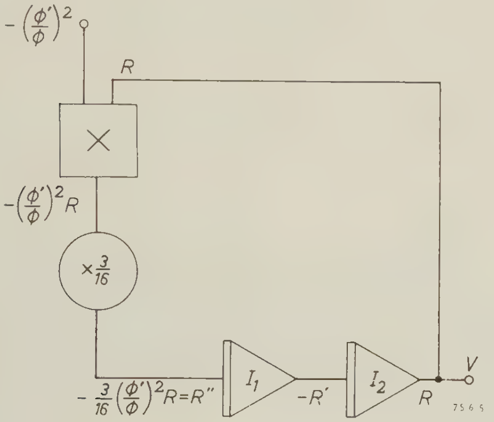
$-\left(\frac{\Phi'}{\Phi}\right)^2$
R
$\times$
$-\left(\frac{\Phi'}{\Phi}\right)^2 R$
$\times\frac{3}{16}$
$-\frac{3}{16}\left(\frac{\Phi'}{\Phi}\right)^2 R = R''$
I_1
$-R'$
I_2
R
V
7565

Fig. 8. Circuit for solving Picht's equation. When the computer is started, R and R' must be given the values $R(0)$ and $R'(0)$. The solution $R(z)$ corresponding to these intial conditions is supplied by the circuit in the form of the varying output voltage $V(t)$.

The sliding contacts and stylus are returned to their starting point, the capacitors in the integrators are discharged, and the machine is ready to produce another solution. For this purpose, different initial values are assigned to R and R'.

Two trajectories plotted in this way can be seen in *fig. 9*.

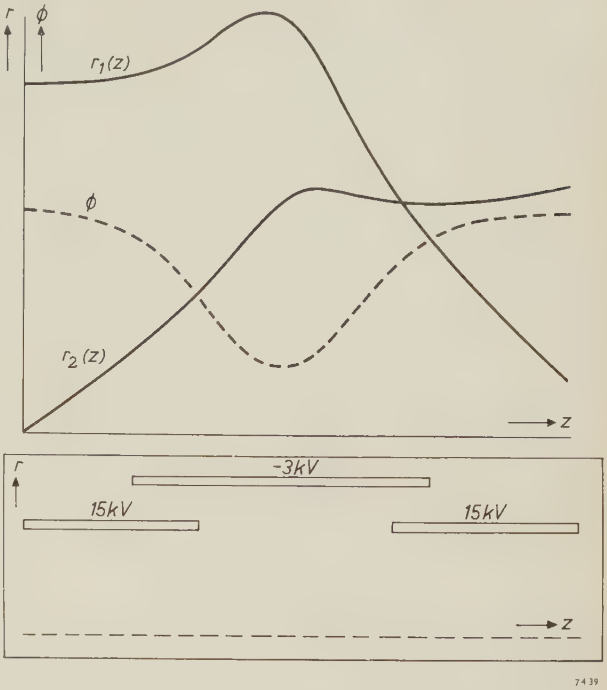

Fig. 9. Two paraxial trajectories $r_1(z)$ and $r_2(z)$ with different initial conditions. Dotted line: variation of the potential Φ on the axis of the electrode system. A half cross-section of the electrode configuration is shown below the graph: the z axes are on the same scale.

Calculation of $(\Phi'/\Phi)^2$

We have already mentioned that the variation of the potential Φ along the axis is found with the aid of a resistance network. In such a network the resistances between all neighbouring network points are dimensioned in such a way that the potential distribution over these points is a good approximation of the potential distribution in an axial cross-section of a rotational-symmetric electrode system. This electrode system is simulated in the network by electrically interconnecting a number of network points and giving them the appropriate potential [10].

The fact that the network does not give a continuous curve for Φ, but only the values of Φ at discrete points, has its consequences. For solving Picht's equation it is, of course, necessary to provide a value of Φ for every value of z. To this end, interpolation is carried out (with the aid of the computer) between the discrete points. This is done by simultaneously determining the values of Φ and Φ' at two successive network points n and $n+1$, while the computer ensures that Φ and Φ' increase linearly with time (and hence with z) from the initial values to the final values in the interval concerned.

This linear interpolation of Φ and Φ' between the points n and $n+1$ (*fig. 10*) is effected in accordance with the formulae:

$$U_n(x) = \Phi_n + (\Phi_{n+1} - \Phi_n)\,\frac{x}{a} \quad . \; . \quad (5a)$$

and

$$W_n(x) = \frac{\Phi_{n+1} - \Phi_{n-1}}{2a} + \left(\frac{\Phi_{n+2} - \Phi_n}{2a} - \frac{\Phi_{n+1} - \Phi_{n-1}}{2a}\right)\frac{x}{a} \quad . \; . \; . \quad (5b)$$

---

[10] For further particulars, see the article under reference [4]. The fact that the "model" of the investigated electrode system can so readily be obtained on the resistance network is one of the great advantages of the network compared with the electrolytic tank: with the latter it takes quite a lot of time to make the electrode models.

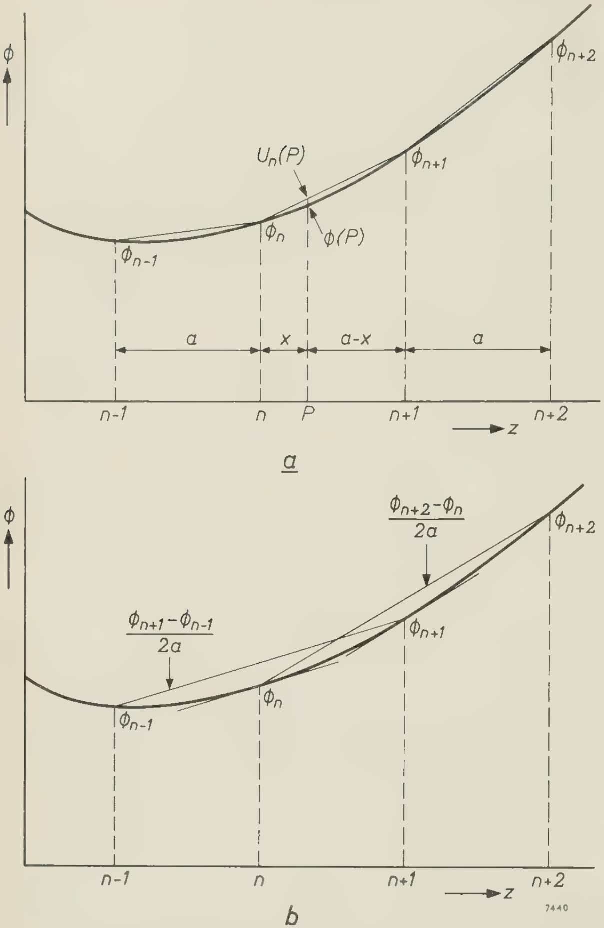

Fig. 10. *a*) Linear approximation of Φ and *b*) of Φ'. Between the points n and $n+1$ we approximate to Φ' by letting the slope of the line $(n-1,\ n+1)$ increase linearly to the slope of $(n,\ n+2)$.

In these expressions Φ_n is the value of $\Phi(z)$ at the point n, $U_n(x)$ is the approximation of $\Phi(z)$ between the points n and $n+1$, $W_n(x)$ is the approximation of $\Phi'(z)$ between the points n and $n+1$, a is the mesh width of the network, and x is the abscissa between the points n and $n+1$, which varies from 0 to a. The derivative Φ' at the point n is approximated, according to eq. (5*b*), by the slope of the line connecting Φ_{n+1} and Φ_{n-1}, as illustrated in fig. 10*b* for an arbitrary curve and an exaggeratedly large mesh width.

In order to show how U_n and W_n are obtained with the computer we write the equations (5) in the following form:

$$U_n = \Phi_n + \int_0^{x/a} (\Phi_{n+1} - \Phi_n)\,\mathrm{d}z\,,$$

$$W_n = \frac{\Phi_{n+1} - \Phi_{n-1}}{2a} + \int_0^{x/a} \frac{\Phi_{n+2} - \Phi_{n+1} - \Phi_n + \Phi_{n-1}}{2a}\,\mathrm{d}z.$$

The circuit with which U_n is computed will be dealt with separately under another heading.

From the formula for W_n it can be seen that the voltages Φ_{n-1}, Φ_n, Φ_{n+1} and Φ_{n+2} have to be simultaneously fed to the computer during the time that the z coordinate is swept between the points n and $n+1$. This simultaneous feed of the four successive voltages is effected with the aid of a telephone selector, shown in *fig. 11*; the circuit diagram is given in *fig. 12*. The wiper arms are all mounted on one shaft, so that they change position simultaneously. In the computer a sinusoidal voltage with a period of one second is generated, and a separate circuit delivers after each period a voltage pulse for the stepwise actuation of the selector. In this way the axis on the network is swept at the rate of one mesh spacing per second. Now the circuit in fig. 8 is dimensioned in such a way that, during the solving of the differential equation, the z axis is swept at a speed which also corresponds to one mesh spacing per second. The above-mentioned time relation between the scanning of the network and the sweeping of the z axis is brought about by the sinusoidal voltage.

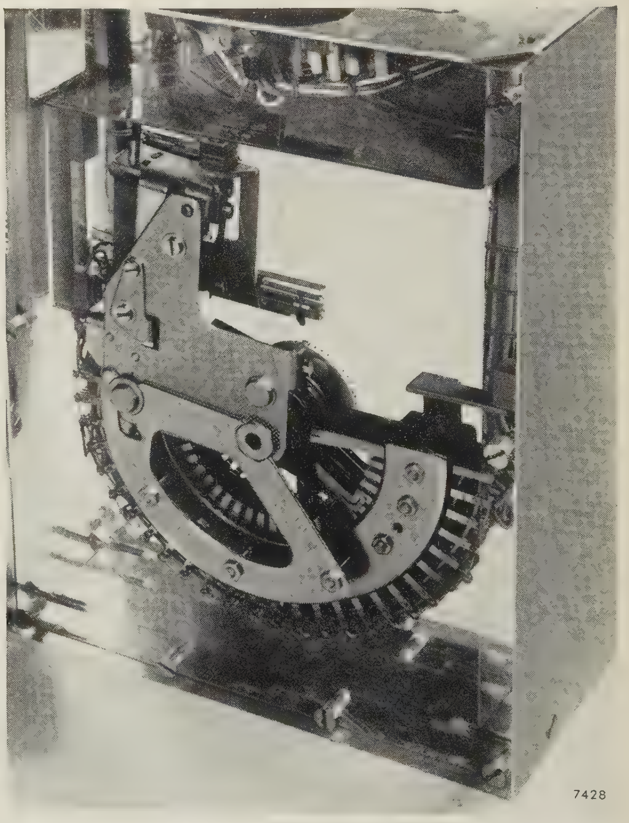

Fig. 11. The four-armed telephone selector (it has five wiper arms but only four are used). There are 26 contacts available on each arc, of which there are two sets of four, mounted one above the other. The four wiper arms, which are mounted on the same shaft, are designed so as to sweep 52 points in each revolution. The selector is mounted in an oil-filled container of transparent plastic, measuring 12×19×23 cm.

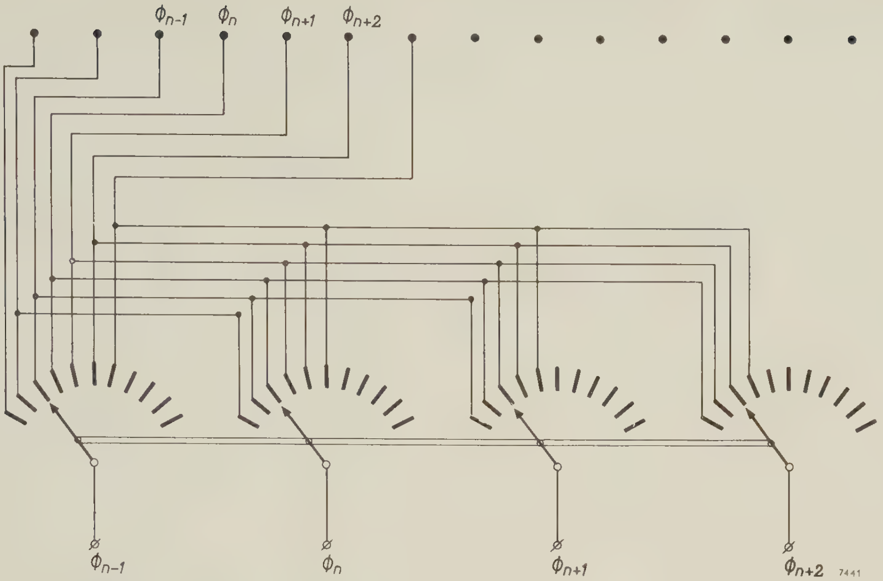

Fig. 12. Circuit diagram of the selector. For clarity, not all contacts are shown. The upper row of points represents a number of axial points of the network.

The four voltages scanned by the selector are fed to the circuit of *fig. 13*, which carries out the interpolation of Φ' between the points n and $n+1$.

At the moment when the x-y recorder begins to trace the trajectory between $n+1$ and $n+2$, the selector jumps to the next position, so that the voltages Φ_n, Φ_{n+1}, Φ_{n+2} and Φ_{n+3} are supplied to the circuit and $W_{n+1}(x)$ is computed. At the same moment as the selector changes position, the capacitor in the integrator (fig. 13) discharges, so that the circuit can begin with a clean slate on the interpolation between $n+1$ and $n+2$.

Network feedback

Fig. 13 shows that the network points switched in by the telephone selector are connected to adders. In fig. 4 it can be seen that, as a result of this, these network points are connected via resistors (R_1, R_2) of about 1 MΩ to a point (p) which has a fixed potential, viz earth potential. The potential Φ in Picht's equation is computed with respect to the potential at the point where the electrons have zero velocity. If we also made this "cathode potential" equal to earth potential, a point of the network having the voltage Φ would be loaded with a current Φ/R_1, which can have a marked effect on the voltage at that point.

To avoid this, the network with its voltage source is made "floating", and negative feedback is applied in such a way that the four points whose potentials are measured, and not the cathode, are on average at earth potential. This is done with the aid of the circuit of *fig. 14*. The operational amplifier A is provided with negative feedback via the resistors of the network, as a result of which the voltage at point *1* is virtually zero. At the moment when the selector has just changed position, $x = 0$, and therefore the voltage at point *2* is zero. It follows, then, that the voltage on *3* must also be zero. This is arranged by means of the amplifier A, which delivers a negative feedback voltage U_t, to be added to all network voltages, such that $\Phi_n + U_t = 0$. In the time between the successive changes of the selector,

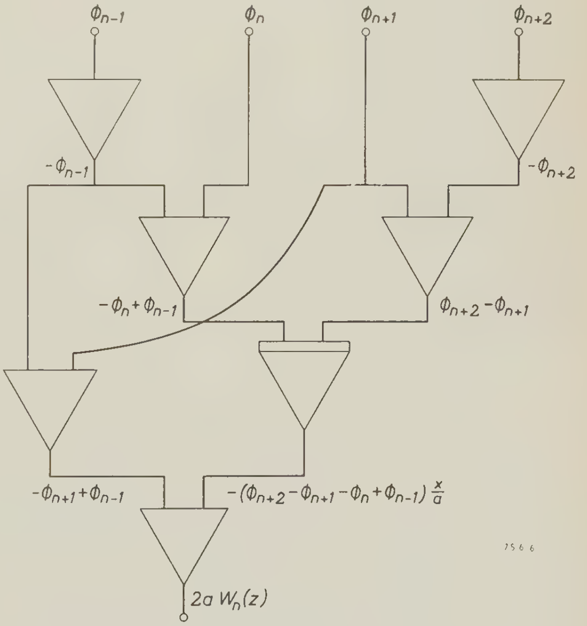

Fig. 13. Circuit for calculating W_n as an approximation of Φ' between the points n and $n+1$.

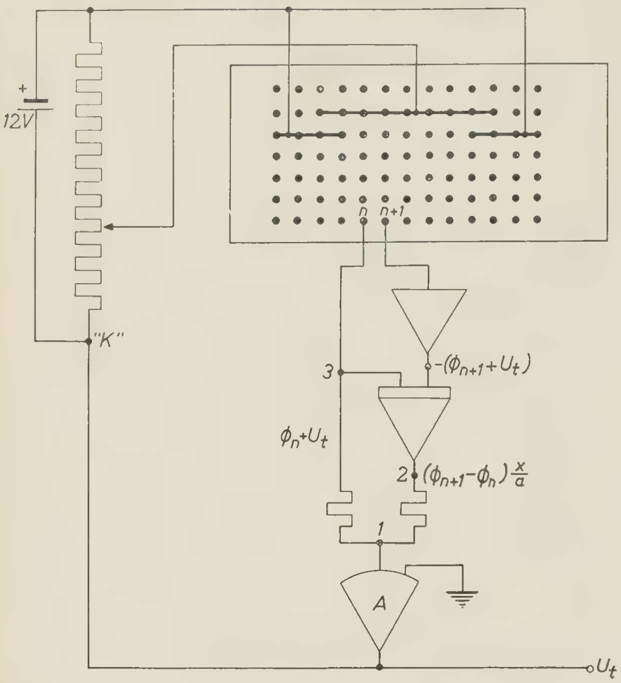

Fig. 14. Negative feedback is applied to the operational amplifier A via the network resistances. The amplifier delivers a negative feedback voltage U_t such that the points between which the potential is measured, n and $n+1$, and not the "cathode" of the network (point "K") are on an average at earth potential. This prevents the computer drawing currents from the network that would disturb the potentials at the network points.

The circuit is so designed that $-U_t$ is exactly equal to U_n, which approximates to $\Phi(z)$ between n and $n+1$.

The voltages at points n and $n+1$ are also conducted to the relevant points in fig. 13. The selector is not shown.

the voltage at *2* increases and, owing to the change of U_t, the voltage at *3* decreases by the same amount. In this way the values of Φ_n and Φ_{n+1} remain near earth potential during a given position of the selector, and unduly large currents cannot be drawn from the network.

The circuit is now so chosen (in particular by including in it the adder and the integrator) as to make the negative feedback voltage U_t exactly the opposite of U_n, which approximates to $\Phi(z)$ between n and $n+1$. This is evident, for when the voltage at *1* is zero,

$$\Phi_n + U_t + (\Phi_{n+1}-\Phi_n)\,x/a = 0,$$

whence

$$-U_t = \Phi_n + (\Phi_{n+1}-\Phi_n)\,x/a,$$

and this, according to (5*a*), is equal to $U_n(x)$.

This negative feedback has no influence on W_n, the determination of which involves only potential differences: these are independent of the potential level of the network.

The circuits in figs 13 and 14 thus deliver the values U_n and W_n, with which Φ and Φ' can be approximated by continuous functions consisting of straight line sections. From these the computer calculates $(W_n/U_n)^2$ as an approximation of $(\Phi'/\Phi)^2$, which function can be fed to the multiplier in fig. 8.

Accuracy of the potential measurement

When the quotient W_n/U_n is computed with the aid of the "divider" (fig. 7) the voltage-division ratio on both potentiometers is governed by U_n. In order to utilize the whole range of the potentiometers, U_n is first multiplied by a number which makes its maximum value only slightly less than that of the reference voltage V_r. (At another point of the circuit it is then necessary to divide by that number.) If now the minimum value of U_n is very much smaller than its maximum value the divider will function very inaccurately at the moment at which this minimum value occurs, for only a few windings of the potentiometer will then be used. Reasonable accuracy is still achieved when the ratio between maximum and minimum values is 20 : 1.

We shall now consider the error caused by approximating Φ and Φ' by U_n and W_n.

In a particular position of the telephone selector the voltages Φ_{n-1} up to Φ_{n+2} are fed to the computer. We wish to know by how much the voltage $U_n(P)$ applied for the point P (fig. 10*a*) differs from the voltage $\Phi(P)$ which follows from the third-degree curve that can be drawn through the four points Φ_{n-1} up to Φ_{n+2}. Although the latter value is not equal to the actual value of $\Phi(z)$ at point P either, it is in any case a better approximation. For calculating the errors in $U_n(P)$ and $W_n(P)$ we therefore assume that the third-degree curve represents the true variation of $\Phi(z)$. This amounts to saying that $\Phi(z)$ can be represented by the first four terms of the Taylor series in the neighbourhood of P (coordinate z_p):

$$\Phi(z)=\Phi(P)+(z-z_p)\Phi'(P)+\tfrac{1}{2}(z-z_p)^2\Phi''(P)+\tfrac{1}{6}(z-z_p)^3\Phi'''(P).$$

Applying this formula to the points $n-1$, n, $n+1$, $n+2$, and writing $z_p - z_n = x$, we find:

$$\begin{aligned}
\Phi_{n-1} &= \Phi(P)-(a+x)\Phi'(P)+\tfrac{1}{2}(a+x)^2\Phi''(P)-\tfrac{1}{6}(a+x)^3\Phi'''(P),\\
\Phi_{n} &= \Phi(P)-x\Phi'(P)+\tfrac{1}{2}x^2\Phi''(P)-\tfrac{1}{6}x^3\Phi'''(P),\\
\Phi_{n+1} &= \Phi(P)+(a-x)\Phi'(P)+\tfrac{1}{2}(a-x)^2\Phi''(P)+\tfrac{1}{6}(a-x)^3\Phi'''(P),\\
\Phi_{n+2} &= \Phi(P)+(2a-x)\Phi'(P)+\tfrac{1}{2}(2a-x)^2\Phi''(P)+\tfrac{1}{6}(2a-x)^3\Phi'''(P).
\end{aligned}$$

Substituting the expressions thus found for Φ_{n-1}, Φ_n, Φ_{n+1} and Φ_{n+2} in equations (5a) and (5b) we find a relation between the approximations $U_n(P)$, $W_n(P)$ and the "true" values $\Phi(P)$ and $\Phi'(P)$:

$$\begin{aligned}
U_n(P) &= \Phi(P) + C_1(x),\\
W_n(P) &= \Phi'(P) + C_2(x).
\end{aligned}$$

The two correction terms, which are functions of x, are given by:

$$\begin{aligned}
C_1(x) &= \tfrac{1}{2}x(a-x)\Phi''(P) + \tfrac{1}{6}x(a-2x)(a-x)\Phi'''(P),\\
C_2(x) &= \tfrac{1}{6}\,(a^2+3ax-3x^2)\Phi'''(P).
\end{aligned}$$

We have calculated the values of C_1/Φ and C_2/Φ' for a particular electrode configuration [11]. The maximum values found were:

$$C_1/\Phi = 0.002 \quad\text{and}\quad C_2/\Phi' = 0.003,$$

representing a maximum error of 0.2% in U_n and 0.3% in W_n.

---

[11] Two identical cylinders in line, and a very small distance apart, their voltage ratio being 20 : 1. As explained above, this is the maximum ratio at which the computer is sufficiently accurate.

These errors should be compared with the errors in the potential due to the finite mesh-width of the network. This error has been determined by Francken [2]) for a given electrode configuration produced on three different scales, and thus for three different mesh numbers [12]). As regards the mesh number, our electrode model on the network corresponds to the above configuration on scale I, for which the error found in the potential is roughly 1%. We see then, that the interpolation of Φ and Φ' is sufficiently accurate. The accuracy can be improved by adopting the imaging mentioned by Francken. Since this involves depicting only half the configuration, the size of the model can be doubled. In that case our electrode model would correspond with Francken's model on scale III, for which an error of 0.5% is given. The errors C_1/Φ and C_2/Φ' are then also smaller, and the linear approximation is accordingly still justified.

Spherical aberration

When a number of paraxial electron trajectories in the field of an electrostatic lens are determined with the set-up described, one can derive from these the positions of the foci and of the principal planes, thus defining the behaviour of the lens as far as focusing is concerned.

Like an optical lens, an electron lens also has its imaging errors (aberrations). It is therefore of considerable importance to be able to determine such aberrations with this equipment. The most serious aberration found in electron beams in the guns of television picture tubes is spherical aberration (*fig. 15*). This is in fact the only aberration that occurs when imaging a point situated on the axis of the lens. The size of the circle of confusion is given by [13]):

$$\Delta r_0 = \frac{5}{64} f r^3 \sqrt{\Phi_0} \int\limits_{-\infty}^{z(F)} \frac{R_n{}^4}{\sqrt{\Phi}} \left[\left(\frac{\Phi''}{\Phi}\right)^2 - \frac{101}{120}\left(\frac{\Phi'}{\Phi}\right)^4 + \right.$$

$$\left. + \frac{13}{3}\left(\frac{\Phi'}{\Phi}\right)^3 \frac{R_n{}'}{R_n} - \frac{6}{5}\left(\frac{\Phi'}{\Phi}\right)^2 \left(\frac{R_n{}'}{R_n}\right)^2 \right] \mathrm{d}z. \qquad (6)$$

Here Φ_0 is the potential of the equipotential space from which the parallel beam proceeds, $z(F)$ is the coordinate of the focus and f the pertaining focal length, and $R_n(z)$ is a normalized paraxial trajectory, i.e. that which comes parallel to the axis from $-\infty$ with $R = 1$. (The normalization, as in the case of V, makes R_n into a dimensionless quantity.)

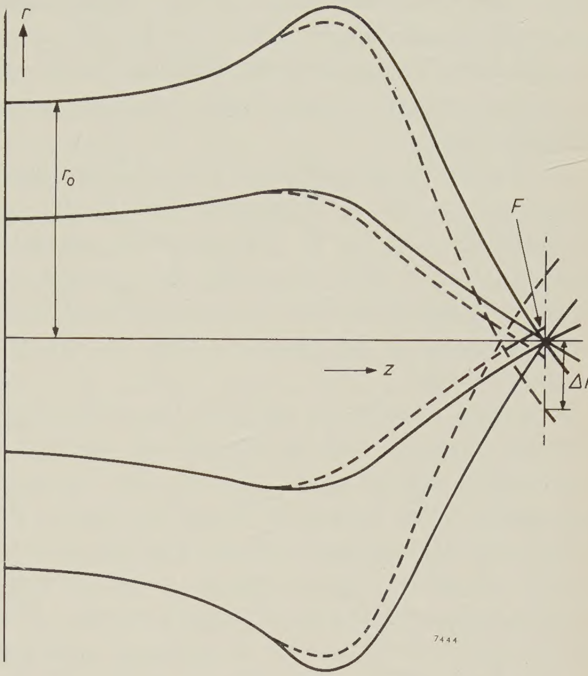

Fig. 15. Spherical aberration in the focusing of electrons. The solid lines represent the theoretical paraxial trajectories which all intersect the axis at the focus. The dashed curves are the actual trajectories when spherical aberration occurs. The outermost trajectories cut the axis nearest to the lens. At the focus a circle of confusion of radius Δr_0 is produced.

To determine Δr_0 with the computer we also need Φ'', for which we make use of the difference between $(\Phi_{n+2} - \Phi_{n+1})$ and $(\Phi_n - \Phi_{n-1})$. The value calculated in this way for each interval n to $n+1$ is practically equal to the mean value of Φ'' in that interval. For calculating the integral the network is again scanned in the same manner. The result of the integration, which is accurate to within 10%, can be read on a voltmeter.

Further applications

To conclude, we shall touch briefly on some other possible applications.

In the case of higher beam currents the mutual repulsion of the electrons has a perceptible influence on the electron trajectories. It has been shown [14]) that the term

$$\frac{1}{4\pi\varepsilon_0\sqrt{2e/m}} \times \frac{I}{\Phi R}$$

should be added in such cases to the left-hand side of Picht's equation, I being the beam current, e the charge on the electron and m its mass. The circuit in the computer must be correspondingly modified.

---

[12]) The "mesh number" is defined as one of the dimensions of the electrode system, divided by the mesh width. Which dimension is taken is immaterial, provided it is consistently adhered to when comparing models on different scales.

[13]) See W. Glaser, Grundlagen der Elektronenoptik, Springer, Vienna 1952, pp. 371 and 675. Formula (6) is obtained by applying the substitution of eq. (2) in the formula given there. The formula is applicable when object and image are located in a field-free space and when the object distance is much greater than the image distance. If the former is much smaller than the latter, as it is in picture tubes (fig. 1) the integral remains the same, but the factor in front of the integral changes.

[14]) See the book mentioned in reference [13]), p. 142.

Where the beam currents are even higher, the potential distribution is influenced by the space charge caused by the electrons. This can be allowed for by the appropriate application of currents to the network points.

The lens action of a magnetic field with rotational symmetry can also be computed with this set-up, provided the field can be defined with a potential function. In this case, of course, the paraxial ray equation differs from that for electrostatic fields [14]) and the circuit in the computer must be adapted correspondingly.

It is also possible to compute the path of an electron moving in both an electrostatic field and a rotational-symmetric magnetic field. For this purpose *two* networks are needed, supplying respectively the electrostatic and magnetic potential distribution to two telephone selectors, one for each network, which simultaneously scan the axial potentials. The path is again calculated with an analogue computer on the basis of the paraxial-ray equation [14]) for combined electric and magnetic fields.

Finally, there is the case where electron trajectories are to be determined in potential fields which vary in the time during which the electron traverses the field. With our set-up it is necessary for this purpose to make the voltages on the electrodes vary with time. The best method is to supply the network with a voltage generated by the computer itself and which varies in accordance with a specific function.

Summary. The effective design of certain electrode systems possessing rotational symmetry (like the focusing lens of a television picture tube) calls for a detailed knowledge of the paraxial trajectories of the electrons. A PACE analogue computer can compute the trajectories as the solutions of a differential equation, Picht's paraxial-ray equation. To make the calculation entirely automatic, the potential variation along the axis of the electrode configuration, as obtained on a resistance network, is scanned by means of a four-arm telephone selector and fed directly to the computer. After discussing the principal component elements of an analogue computer, the authors explain how the computer derives a continuous function by interpolation from the discrete potential values obtained from the resistance network, and describes the process of solving the potential equation. The accuracy of the interpolation is also examined. The same set-up can be used to determine the spherical aberration of the electron lens.

ABSTRACTS OF RECENT SCIENTIFIC PUBLICATIONS BY THE STAFF OF N.V. PHILIPS' GLOEILAMPENFABRIEKEN

Reprints of those papers not marked with an asterisk * can be obtained free of charge upon application to Philips' Electrical Ltd., Century House, Shaftesbury Avenue, London W.C. 2, where a limited number of reprints are available for distribution.

2918: P. Westerhof and E. H. Reerink: Investigations on sterols, XVIII. The synthesis and properties of some hydroxylated $9\beta,10\alpha$-pregnanes (Rec. Trav. chim. Pays-Bas **79**, 1118-1125, 1960, No. 9/10).

The synthesis of a number of $9\beta,10\alpha$-pregnanes and $9\beta,10\alpha$-androstanes has already been described (these abstracts, Nos **2881** and **2882**). The synthesis of the 17α-hydroxy derivatives of $9\beta,10\alpha$-progesterone and of 6-dehydro-$9\beta,10\alpha$-progesterone, and some acylates of these compounds, is now described in the present publication. Tests on rats, mice and rabbits show that the acylates have a strong progesterone-like effect when administered subcutaneously, while they show the same effect on rabbits when orally administered.

2919: H. B. G. Casimir: A note on multipole radiation (Helvetica Phys. Acta **33**, 849-854, 1960, No. 8).

The expansion of a radiation field in a series of electric and magnetic multipole fields has already been investigated by several authors. Bouwkamp and Casimir (1954) showed that this expansion can conveniently be obtained by means of "Debye potentials". The use of group theory was avoided in reaching this result. It is now shown that the use of group theory leads to the same result, in a logical and straightforward way.

2920: C. Haas: The diffusion of oxygen in silicon and germanium (Phys. Chem. Solids **15**, 108-111, 1960, No. 1/2).

Starting from a simple model for the location of O atoms in crystals of Si and Ge, and from the assumption that internal friction and diffusion are both governed by the same relaxation process, the diffusion coefficient for oxygen in these elements, $D = D_0 \exp -(U/kT)$, is calculated from experimental data on internal friction. The results are for

Si: $D_0 = 0.21$ cm^2/sec, $U = 2.55$ eV; for Ge: $D_0 = 0.17$ cm^2/sec, $U = 2.02$ eV. The calculated values are in satisfactory agreement with the available experimental data.

2921: M. J. Sparnaaij: Gas adsorption and surface charge density of germanium surfaces (Phys. Chem. Solids **14**, 111-116, 1960).

Investigation of the effect of the presence of discrete charges on the surface of germanium crystals on the adsorption of gases such as argon. This effect is to be expected at charge densities of 10^{13}-10^{15} elementary charges per cm^2. Below this range, the effect will be too slight, and above the individual fields all merge into one. The Van der Waals forces which hold the gas atoms on the surface are compared with the polarization energies calculated in this publication for various charge densities. The theoretical results are compared with experimental determinations of the difference in the chemical potentials of argon adsorbed on non-oxidized and oxidized Ge. The difference is of the expected order of magnitude, and the charge density of 10^{14}-10^{15}/cm^2 thus found also agrees with the results obtained by Green on the change in the contact potential on oxidation.

2922: W. Albers, C. Haas and F. van der Maesen: The preparation and the electrical and optical properties of SnS crystals (Phys. Chem. Solids **15**, 306-310, 1960, No. 3/4).

Single crystals of SnS were prepared by heating a stoichiometric mixture of the components in vacuo to about 900 °C. The melting point is 880 ± 5 °C. Rhombic single crystals were prepared by passing a powdered sample at 420 °C in vacuo slowly through a melting zone (900 °C). Platelets measuring e.g. $2 \times 0.5 \times 0.3$ cm can be obtained by cleaving such crystals perpendicular to the *c*-axis. It follows from measurements of the Hall effect that the crystals are *P*-type semiconductors with 10^{17}-10^{18} holes per cm^3. The mobility μ_p of the holes depends on the temperature, with a maximum at about 200 °K. At room temperature, $\mu^\mathrm{p} = 65$ cm^2/V sec. Preliminary measurements show that the specific conductance parallel to the *c*-axis is about 6 times smaller than that in a direction perpendicular to this. The crystals are completely opaque for radiation with a wavelength of less than 1 μm, which indicates that the band gap is 1.07 ± 0.04 eV. For wavelengths greater than 1 μm the absorption coefficient is proportional to λ^2. Application of Drude's equation gives an effective mass of the holes equal to 0.4 of the mass of an electron.

2923: J. Hornstra: Dislocations, stacking faults and twins in the spinel structure (Phys. Chem. Solids **15**, 311-323, 1960, No. 3/4).

The slip plane in crystals with the spinel structure is probably the (111) plane, in analogy with the (0001) slip plane in corundum-type crystals. This is confirmed by an observation of twinning during deformation, which can be regarded as a process in which partial dislocations with a (111) slip plane take part. Dislocations with this slip plane probably consist of 4 partial dislocations separated by 3 regions of stacking faults. The structure of these stacking faults is compared with that of the perfect spinel lattice. During slip, the cations move in a direction different from that of the oxygen ions. This process is discussed in some detail for the case of 4-coordinated cations. Another type of stacking fault shows similarities with the olivine lattice. Two possible configurations of the (111) twin boundary are discussed.

2924: J. Th. G. Erhardt: Technische beschermingsmaatregelen tegen warmtestraling (Ingenieur **72**, G.78 - G.88, 1960, No. 51). (Protective measures against thermal radiation; in Dutch.)

Personnel (and equipment) in the vicinity of e.g. a furnace can be protected against the heat by means of radiation screens. The temperature of and thermal radiation from the outer layer of a number of types of reflecting screens have been calculated as functions of the temperature of the body to be screened off. In order to check the practical utility of these calculations, the results were compared with experiment. The agreement was good; moreover, the calculated values were on the high (i.e. the safe) side. Finally, a few remarks are made about the use of radiation screens in practice.

2925: L. J. van der Pauw: An analysis of the circuit of Dauphinee and Mooser for measuring resistivity and Hall constant (Rev. sci. Instr. **31**, 1189-1192, 1960, No. 11).

Measurements of the resistivity and Hall coefficient of semiconductors with the aid of the circuit of Dauphinee and Mooser can show certain systematic errors due to capacitive effects in the switch. The magnitude of these errors is estimated, and it is shown how they can be eliminated with the aid of trimming capacitors in the right places and a suitably chosen switching programme. The sensitivity of the circuit is also calculated.

2926: H. J. Eichhoff and N. W. H. Addink: Untersuchungen zur Übertragbarkeit spektrochemischer Verfahren mit vollständiger Verdampfung (VIII. Colloquium Spectroscopicum Internationale, Lucerne 14th-18th Sept. 1959, Ed. H. Guyer, pp. 89-92; Sauerländer, Aarau (Switzerland) 1960). (Investigations of the transferability of spectrochemical methods based on complete evaporation; in German.)

5-10 mg of a material can be accurately spectrochemically analysed by completely evaporating the sample in a DC carbon arc. Careful preparatory work is needed to work out the exact method of analysis for the sixty or so elements for which it can be used. If however the method is once worked out for one type of spectrograph, it is relatively easy to change over to another type of instrument: all that needs to be done is to determine the conversion factors. Values of these factors are given for various spectrographs in the wavelength region 2500-3500 Å. For prism instruments, the factor is equal to 1 ± 0.1 over the whole range of wavelengths, but with grating instruments it depends strongly on the wavelength, and on the "blaze" of the grating. Analytical results are given.

2927: H. Bienfait: Management policy of the Philips Research Laboratory (Spring Meeting of the Industrial Research Institute, Virginia Beach, 8th-11th May 1960, pp. 201-215).

A survey of the history of the development and the organization of the Philips Research Laboratories, and also of the various steps taken to ensure a good scientific atmosphere. The relationship between the Research Laboratories and the development laboratories is discussed. The article ends with a look into the future.

2928: J. C. Francken and J. van der Waal: Residual gases in picture tubes (Vacuum **10**, 22-26, 1960, No. 1/2).

See Philips tech. Rev. **23**, 122, 1961/62 (No. 4).

2929: J. H. N. van Vucht: The Ceto getter — its chemical structure and hydrogen gettering properties (Vacuum **10**, 170-177, 1960, No. 1/2).

An investigation of the absorption of hydrogen by Th_2Al and of the reaction products formed. The equilibrium pressure of hydrogen above Th_2Al is measured as a function of the temperature and of the amount of hydrogen absorbed. The structure of the reaction products is studied by means of X-ray diffraction, neutron diffraction and nuclear magnetic resonance. The kinetics of the absorption are also studied, for the case where the surface of the Th_2Al is covered with oxygen (inactivated surface). Autocatalysis is observed to occur; a simple explanation is given for this effect. This investigation arose out of the study of the non-evaporating getter "Ceto", which has important uses in industry. This getter has the same structure as Th_2Al, but some of the thorium atoms are replaced by cerium and lanthanum. See also **R 411.**

2930: W. K. Westmijze: Eigenschaften und Anwendungen von Magnetkernen in der Messwertverarbeitung (Elektrotechn. Z. **A 81**, 779-783, 1960, No. 22). (Properties and use of magnetic cores in data processing; in German.)

The processing of data obtained as the results of measurements plays an important role in modern control engineering. It is often necessary to store the data, or quantities calculated therefrom, in a memory until they are needed again. For many applications it must be possible to place the data in the memory, and to retrieve them, very rapidly. The properties of magnetic cores in this connection are discussed in this article, which ends with a simple example of the uses to which a magnetic-core memory can be put.

2931: J. A. M. Dikhoff: Cross-sectional resistivity variations in germanium single crystals (Solid-state electronics **1**, 202-210, 1960, No. 3).

Germanium single crystals often show an undesired variation in the dope concentration. It has been found that flat facets can develop on an otherwise curved growth interface during the growth of the crystals. These facets coincide with {111} planes. The reason for the above-mentioned variation in the dope concentration is that the segregation constants of various elements differ for the flat and the curved parts of the growth interface. Methods of producing more uniform crystals are discussed.